



## Model-driven design of bioactive glasses: from molecular dynamics through machine learning

Maziar Montazerian, Edgar D. Zanotto & John C. Mauro

**To cite this article:** Maziar Montazerian, Edgar D. Zanotto & John C. Mauro (2020) Model-driven design of bioactive glasses: from molecular dynamics through machine learning, International Materials Reviews, 65:5, 297-321, DOI: [10.1080/09506608.2019.1694779](https://doi.org/10.1080/09506608.2019.1694779)

**To link to this article:** <https://doi.org/10.1080/09506608.2019.1694779>



Published online: 06 Dec 2019.



Submit your article to this journal [↗](#)



Article views: 886



View related articles [↗](#)






View Crossmark data [↗](#)



Citing articles: 21 View citing articles [↗](#)

## Model-driven design of bioactive glasses: from molecular dynamics through machine learning

Maziar Montazerian <sup>a</sup>, Edgar D. Zanotto <sup>a</sup> and John C. Mauro <sup>b</sup>

<sup>a</sup>Department of Materials Engineering (DEMa), Center for Research, Technology and Education in Vitreous Materials (CeRTEV), Federal University of São Carlos (UFSCar), São Carlos, Brazil; <sup>b</sup>Department of Materials Science and Engineering, The Pennsylvania State University, University Park, PA, USA

### ABSTRACT

Research in bioactive glasses (BGs) has traditionally been performed through trial-and-error experimentation. However, several modelling techniques will accelerate the discovery of new BGs as part of the ongoing endeavour to ‘decode the glass genome.’ Here, we critically review recent publications applying molecular dynamics simulations, machine learning approaches, and other modelling techniques for understanding BGs. We argue that modelling should be utilised more frequently in the design of BGs to achieve properties such as high bioactivity, high fracture strength and toughness, low density, and controlled morphology. Another challenge is modelling the biological response to biomaterials, such as their ability to foster protein adsorption, cell adhesion, cell proliferation, osteogenesis, angiogenesis, and bactericidal effects. The development of databases integrated with robust computational tools will be indispensable to these efforts. Future challenges are thus envisaged in which the compositional design, synthesis, characterisation, and application of BGs can be greatly accelerated by computational modelling.

### ARTICLE HISTORY

Received 13 February 2019  
Accepted 14 November 2019

### KEYWORDS

Bioactive glass; biomaterials; modelling; simulation

### Introduction

Theoretical and computational modelling are becoming ubiquitous in materials research. Modelling can assist greatly in reducing the timescales required for the translation of basic research into advanced materials and manufacturing [1]. Different governmental initiatives have been launched aiming to improve current modelling capabilities and increase industrial competitiveness [2]. For example, in 2011, U.S. President Barack Obama announced the Materials Genome Initiative (MGI), promising a renaissance in the development of new industrial materials. The U.S. federal government invested over US \$250 million to coordinate research activities in materials science and to accelerate the process of discovering new materials for potential future commercialisation [3]. In this framework, different programmes initiated synergetic collaboration among experimental and theoretical materials scientists, data scientists, and experts from adjacent fields. Glasses are among those high-tech materials being targeted for new advances following the materials genome approach.

Glass is defined as

a nonequilibrium, noncrystalline condensed state of matter that exhibits a glass transition. The structure of glasses is similar to that of their parent supercooled liquids (SCL), and they spontaneously relax toward the SCL state. Their ultimate fate, in the limit of infinite time, is to crystallize. [4]

One of the most well-known diagrams in glass science, the enthalpy versus temperature plot, is shown in **Figure 1**. The different regions in the figure are: (i) The thermodynamically stable liquid state above the melting point or liquidus temperature,  $T_m$ . (ii) The metastable supercooled liquid (SCL) state, which exists between  $T_m$  and the glass transition temperature,  $T_g$ . The SCL eventually crystallises (green arrows) after a certain time. (iii) Glasses exist below the glass transition temperature,  $T_g$ . They are thermodynamically unstable and spontaneously relax toward the supercooled liquid state at any non-zero temperature (grey arrow in **Figure 1**). The glass transition takes place around  $T_g$ , the temperature where the experimental or observation time is similar to the average structural relaxation time of the SCL. On the heating path, a glass changes to a SCL at  $T_g$ . At any positive temperature, above or below  $T_g$ , for sufficiently long times, any SCL or glass relaxes and then eventually crystallises (arrows in **Figure 1**). (iv) Crystals are true solids that are thermodynamically stable below  $T_m$  with well-ordered atomic structures at short, medium, and long-range scales. We stress from the beginning that, due to their crystal-free structure, glasses are particularly amenable to several atomic-scale modelling techniques, since many of their properties depend primarily upon their chemical composition and not microstructural effects. In other words, there are direct *composition-property relationships, and the key*

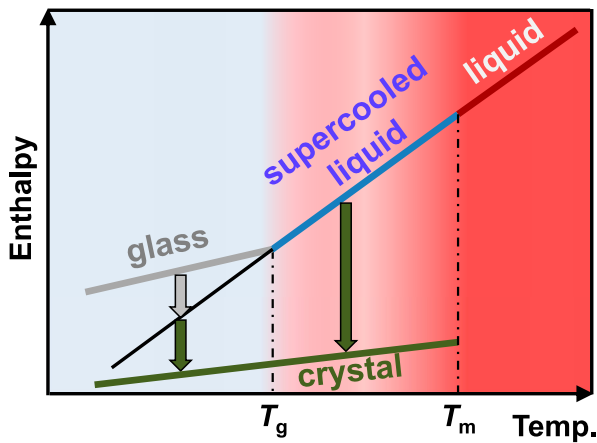


**Figure 1.** Schematic enthalpy versus temperature plot for glass-forming materials showing four distinct states: liquid, supercooled liquid, glass, and crystal.  $T_m$  = melting point or liquidus temperature,  $T_g$  = glass transition temperature (reproduced with permission from Ref. [4]).

challenge is to find them [4,5]! And there are ‘zillions’ of possible compositions to be explored. In a useful exercise, Zanotto and Coutinho [6] estimated that  $10^{52}$  glasses could be made by combining 80 friendly elements of the periodic table in 1% molar steps.

Conventional empirical (or semi-empirical) approaches for developing new materials and characterising their properties are expensive and time-consuming. Recently, modelling is emerging as a significant component of research in glass science, inline with the MGI effort [7,8]. To achieve this goal, it is necessary to utilise an extensive set of techniques, from purely empirical, brute-force computer methods (such as machine learning (ML)), to those incorporating detailed fundamental physics, such as molecular

dynamics (MD). Figure 2 provides an overview of various modelling and simulation methods for predicting the properties of glassy materials. A variety of models are available, from purely empirical models that rely on the mathematical fitting of experimental data, to *ab initio* methods built on a detailed description of the material’s electronic structure. Classical molecular dynamics (CMD) simulations have proven to be especially helpful for understanding the atomic structure, dynamic processes (diffusion, viscous flow, relaxation, liquid-liquid phase separation, and crystallisation) and several other properties of glasses [7,8]. While many of these modelling approaches are standard techniques that can be applied to any class of material, other methods have been developed specifically for modelling disordered systems such as glasses. For example, topological constraint theory (TCT) is an approach that describes the connectivity of the disordered glassy network, an especially useful technique for use in the design of new glass compositions, since accurate yet straightforward models can be derived for a diverse range of properties [9]. Constraint-based models for the temperature and composition dependence of viscosity are already in routine use in industry. While accurate models exist for a variety of properties, *liquidus temperature and crystallization behaviour remain a very significant challenge* that would benefit from increased attention from academic research groups [7–9].

The appropriate choice of modelling technique depends on the nature of the system under study, the desired properties to calculate, the availability of quality data, and the level of physical understanding governing the relevant structure-property relationships in

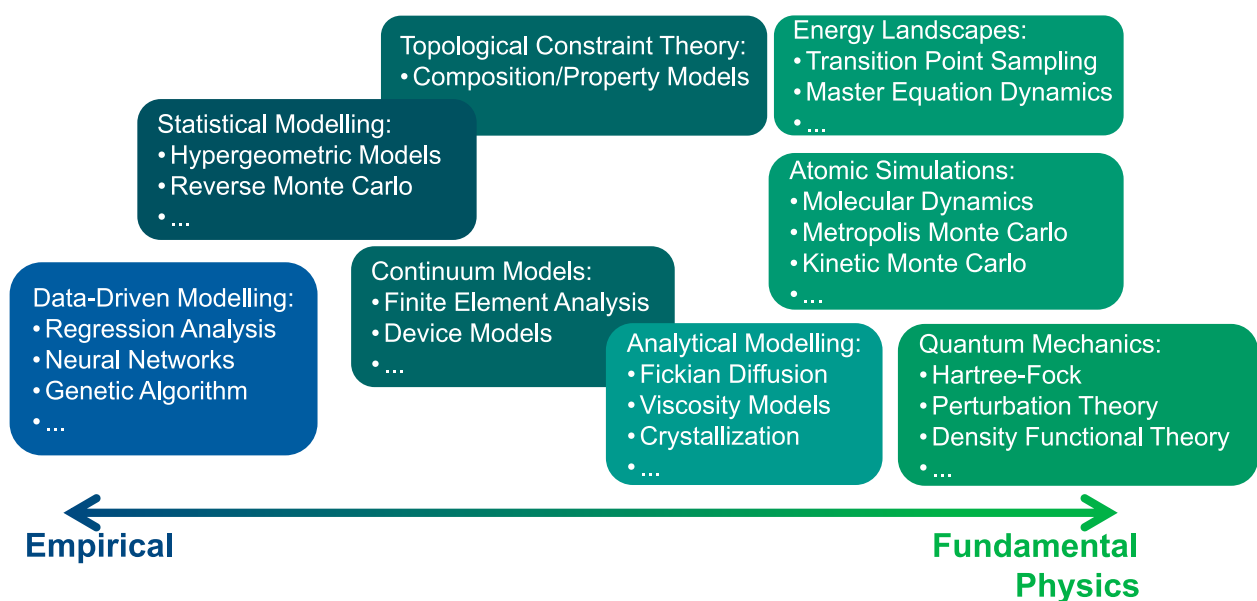


**Figure 2.** Decoding the ‘glass genome’ involves the use of a wide range of modelling tools, from empirical to theoretical approaches that account for the detailed underlying physics and chemistry. Typically, the use of a combination of modelling approaches considering different levels of physics can provide the most significant insights and accurate predictions (reproduced with permission from Ref. [7]).

that system. Often a combination of multiple modelling approaches that incorporates different levels of physics can yield a more comprehensive picture of any given property. Of course, all models need to be validated by experiments, and they are often most effective when developed in close collaboration with experimentalists. Models incorporating a higher degree of physical understanding are preferable for accurately predicting properties outside of the compositional ranges used for fitting and validation [1,8]. Through a combination of different approaches, from atomistic through empirical modelling, Mauro et al. [9] have contributed to ‘decoding the glass genome’ and efficiently designing the famous Gorilla® Glass, Corning’s thin, damage-resistant glass [9]. This product has been used in several billion devices, including smartphones, tablets, smartwatches, automotive glass, and in interior architecture [10].

The importance and the huge impact of the discovery of bioactive glasses (BGs) by Larry Hench [11] in 1969, including the chronology of scientific and technological advances, prospects and challenges for the future, have been elaborated in many original and review papers. We searched the Scopus database using the words [‘bioactive and glass\*’ or ‘bioglass’] in the article title and found 105 review papers published in the last 25 years, including 10 in 2018. They discuss the compositions, properties, and applications of BGs. Some diverse and unique capabilities of BGs, reviewed in Refs. [12–39], include: bone-bonding ability [12–14], bone regeneration [15,16], regeneration of soft tissues [17–22], angiogenesis property [23], bactericidal effect [24], gene expression [25], therapeutic ion release [26–28], drug delivery capability [29–32], functionalisation, e.g. tough bioactive implants (e.g. bio glass-ceramics) [33,34], coatings [35], composites [36], hybrids [37], and cancer treatment [38,39]. Finally, in addition to several scientific journals dedicated to biomaterials, there is even a dedicated periodical called *Biomedical Glasses* [40].

The bioactivity of a material is characterised by their ability to stimulate a favourable response from the body, which in BGs mainly relies on the controlled release of soluble species, such as calcium, sodium, phosphorus, silicon, and boron [12]. For example, Figure 3 illustrates how the release of therapeutic ions from a BG structure into the surrounding environment is considered one of the main reasons for its biological effects [41]. Several trace elements have been successfully incorporated into glass structures for improving their therapeutic effects, including osteogenesis, angiogenesis, bactericidal activity, and anti-inflammation properties. The release profile of the depicted ions in Figure 3 depends on various parameters, such as glass composition, surface topography, porosity, particle size and chemical environment. The composition determines the chemical degradation

rate of the glass in a specific environment and, therefore, controls the ion release rate into the biological environment [26,41]. As an example, it has been proposed that the incorporation of certain ions, such as silver ( $\text{Ag}^+$ ), zinc ( $\text{Zn}^{2+}$ ), copper ( $\text{Cu}^+$  and  $\text{Cu}^{2+}$ ), cerium ( $\text{Ce}^{3+}$  and  $\text{Ce}^{4+}$ ), and gallium ( $\text{Ga}^{3+}$ ) into the structure of BGs and their controlled release is a viable strategy for inhibiting bacterial growth and reproduction [31,42].

In writing this review paper, we first surveyed articles in which any type of modelling of BGs has been addressed. To our surprise, we found that the direct modelling of BG compositions was primarily limited to MD simulations (Second Section), plus a handful of publications on the application of ML-based approaches and meta-analysis (Third Section). This limited number of modelling studies of BGs is not commensurate with the MGI programme and with the expectations of the community. Therefore, in Perspectives, we suggest some promising modelling approaches such as TCT and artificial neural networks (ANNs) for glass property characterisation and related biological response. Finally, based on this review of current modelling approaches, in Conclusions, we offer a view to the future for glass and biomaterials science, their successes, limitations, and challenges.

## MD simulations

In glass science, the combination of laboratory experiments and computer simulations can provide deeper, microscopic physical insights into the structural details and dynamic processes of vitreous materials for confirming or refuting theories and understanding and predicting properties. In particular, atomistic simulations have proved invaluable for determining the structure of many glasses and glass-forming liquids [43,44]. Computational power has increased dramatically over the past few decades, enabling researchers to simulate larger and larger systems (up to roughly a billion particles) or over longer timescales (up to microseconds for some systems). Also, a number of new simulation techniques have allowed the calculation of many thermal, mechanical, and kinetic properties of glass. Indeed, modelling has proved essential for developing a fundamental understanding of structure-property relationships, and it promises to play an indispensable role in the development of new glass compositions with the desired combination of properties [8]. In this section, we provide a critical overview of MD simulations and offer some thoughts about the future of this method for modelling of complex multicomponent glasses, including BGs.

MD is the most commonly used method for performing atomistic simulations of glasses, and BGs are no exception. For example, MD simulations are used to model glass water interaction, which is an important



*initio* MD (AIMD) has been used. In this method, forces are calculated using quantum mechanical methods. Such a first-principles approach is an excellent way to incorporate detailed electronic effects in the MD model; hence, AIMD has much broader applicability than classical MD. However, due to the extremely demanding calculations, only relatively small systems (<1000 particles) can be modelled in a reasonable timescale [49,51]. Therefore, the maximum affordable size and time scales of *ab initio* MD simulations are far too small to observe the evolution of, e.g. sol-gel synthesis of nano-sized bio-glasses and their reactivity over relatively long time scales [52,53].

On the other hand, classical MD can simulate larger system sizes and longer timescales, but most standard force fields are not suitable for describing the rapidly changing bonding configurations and charge distributions of reactive processes. Glass dissolution typically happens at a sub-nanometer length scale, with elementary dynamical events lasting a few picoseconds. This is the timescale for attempting to jump over a barrier, but with so many unsuccessful jumps, the actual time scale of dissolution is much longer. Also, the dissolution process involves chemical reactions, which require different force fields. To address this problem, MD simulations of the silica polymerisation, for example, have employed 'reactive' force fields, which were capable of realistically reproducing the rupture and formation of covalent chemical bonds during the course of the reactions, such as dissociation of OH<sup>-</sup> and silanol groups in water, incorporation of hydroxyls in the silica network and their condensation to Si-O-Si bridges, and so forth. The application of reactive force fields (such as ReaxFF) in MD simulations of glasses is well demonstrated and has been reviewed recently [52-56].

Other AIMD methods, such as the Car-Parrinello molecular dynamics (CPMD) and Born-Oppenheimer molecular dynamics (BOMD), have also enabled modelling of silicate glasses with higher accuracy, e.g. challenging the difficult issues in modelling of surface reactivity and dynamic processes in glasses. Glass scientists frequently use classical MD with empirical potentials to obtain an initial structure and then switch to *ab initio* using the classical structure as 'starting state.' This approach limits the investigation of short-range features or properties that have mainly local (short-range) character. However, a full *ab initio* approach could solve the latter two problems and provide a view of some dynamical and structural features of multicomponent BGs. Compared with the mixed *classical/ab initio* approach, the full *ab initio* procedure demands significantly more computational resources [49-51]. All in all, appropriate force fields are currently available that allow one to access relatively large system sizes, on the order of ~10<sup>9</sup> atoms for monoatomic systems and ~10<sup>6</sup> atoms for multicomponent with a high level of accuracy.

Models of these sizes, spanning lengths between two and a few tens of nanometer, are necessary to extract structural properties relevant, for example, for glass dissolution with a high statistical accuracy [50,51].

We should emphasise that this topic has been partly reviewed in papers and book chapters by Tilocca [50,51], Christie et al. [57], and Pedone and Menziani [58]. They have highlighted that the physicochemical behaviour of BGs in a physiological environment can indeed be investigated using computer simulations. Here, we elaborate on all relevant (old and new) findings on this particular topic and discuss the challenges ahead. Up to now, MD simulations have been employed to model *nano bio-glasses*, the *structure, ion migration in BGs*, and to find descriptors of the *chemical degradation* of BGs. In the following, we critically review those articles and point to relevant topics that warrant further research.

### Structure of BGs

The structure of the pioneering material, 45S5 Bioglass<sup>®</sup>, which is composed of Na<sub>2</sub>O-CaO-P<sub>2</sub>O<sub>5</sub>-SiO<sub>2</sub>, has been simulated by Tilocca [59-61]. The modelled structure (involving melt-quenched systems containing ~10<sup>3</sup> atoms at cooling rates of 5-10 K ps<sup>-1</sup>) is dominated by very short silicate chains containing 2 to 4 monomers (silicon-oxygen tetrahedra) corroborating its low glass-forming ability and high solubility. The modelled structure, besides statistical fluctuations, is essentially unaffected by the cooling rate. Although the simulation boxes were varied by a factor of 32, the distributions of silicate chain lengths remained almost constant. The only apparent effect of a smaller box size was a slightly higher fraction of the smallest (dimer and trimer) chain fragments [60-62]. This finding conveyed the message that the medium-range structural order of BGs, extracted from models of silicate and phosphate glasses through conventional MD simulations, are generally reliable. Therefore, the CPU-demanding task to access larger sizes ( $N > 10^5$  atoms) or slow cooling rate (<10<sup>-2</sup> K ps<sup>-1</sup>) is, in most cases, unnecessary [60,63].

Pedone et al. [64] then used an integrated computational method which couples CMD simulations with periodic density functional theory (DFT) calculations to generate the theoretical solid-state NMR spectra of <sup>17</sup>O, <sup>23</sup>Na, <sup>29</sup>Si, and <sup>31</sup>P isotopes when studying 45S5 Bioglass<sup>®</sup>. Their results provided valuable insights into several open questions regarding the atomic-scale structural details of this glass. In particular, they showed that the host silica network, described by the Q<sup>n</sup> distribution, consists of chains and rings of Q<sup>2</sup> (67.2%) SiO<sub>4</sub> tetrahedra cross-linked with Q<sup>3</sup> (22.3%) species, and terminated by a smaller quantity of Q<sup>1</sup> (10.1%) species. No Si-O-P bridges were detected by either the <sup>31</sup>P NMR or <sup>17</sup>O NMR

experiments. Isolated orthophosphate units can hence form nano-domains with sodium and calcium cations that diminish the role of these ions as modifiers in the silicate network. The experimental and theoretical results showed a mixture of Na and Ca cations surrounding the non-bridging oxygens (NBOs) [64].

Stevensson et al. [65] also found through combined NMR and MD simulations that the dispersion of phosphate ions remains independent of the silicate network polymerisation and is almost independent of the P content of the glass in the compositional space of 1–6 mol-%  $P_2O_5$  and silicate network connectivities up to 2.9, which represents the average number of bridging oxygens per  $SiO_4$  tetrahedron. These results disagree from the findings of Linati et al. that detected a small amount of Si–O–P links in glasses with low  $P_2O_5$  content, and that at high  $P_2O_5$  concentration the Si–O–P bridges became important [66]. Recently, Bhaskar et al. [67] have addressed this issue by considering the effects of the cooling rate used during the preparation of standard 45S5 Bioglass®. They used MD simulations and NMR experiments to investigate the structure of the glass synthesised using cooling rates ranging over several orders of magnitude. The results from simulations are in very good agreement with experimental data, provided that they are extrapolated toward lower cooling rates achieved in experiments. Their findings highlight that previously reported inconsistencies between simulations and experiments stem from the huge differences in cooling rate, thereby addressing one of the longstanding questions on the structure of 45S5 BG, viz. the existence of Si–P avoidance behaviour, which may be key in controlling the bioactivity of this glass.

Recently, Lu et al. [68] prepared a series of  $B_2O_3$ -substituted  $SiO_2$  in 45S5 BGs and performed *in vitro* biomineralisation tests. Formation of hydroxyapatite (HAp) was observed on the glass surfaces of all compositions after 3 weeks, but HAp formation on glasses with higher boron oxide was slower. MD simulations were employed to complement the experimental findings to understand the structural changes due to  $B_2O_3$  to  $SiO_2$  substitution by using partial charge composition-dependent potentials. The overall network connectivity of Si obtained from MD simulations increased with increasing boron content: from 2.06 for 45S5 to 2.45 for a pure borate glass (Figure 4). Therefore, this increase of network connectivity with boron concentration is at least partially responsible for the delayed HAp formation *in vitro* after inducing boron in this glass [68].

Mead and Mountjoy [69] have reported on MD simulations of the first detailed models of the local atomic structure of *gel-derived* bioactive  $SiO_2$ –CaO glasses, with the composition of  $Ca_xSi_{1-x}O_{2-x-y}(OH)_{2y}$ ,  $0 \leq x \leq 0.5$  and  $y = 0.2$ . The MD models were in

satisfactory agreement with experimental results and showed the expected reduced network connectivity of tetrahedral silica due to the presence of Ca and hydroxyl groups. Ca ion coordination number (CN) was  $\sim 6$  for a Ca mole fraction of  $x = 0.5$ , mostly located near nonbridging oxygens, with a small contribution from bridging oxygens. The hydroxyl groups bonded to Si forming Si–O–H bonds, but there is also a substantial contribution to the Ca coordination from hydroxyl groups, which reduced the amount of non-bridging oxygens bonded to Si. The Ca distribution for  $x = 0.5$  was similar to that in melt-quenched  $CaSiO_3$  glass obtained from neutron diffraction experiments. For  $x$  around  $\sim 0.1$ , clustering of Ca was observed, greater than expected for a random distribution. The role of hydroxyl groups in coordination to Ca was supposed to enhance the dissolution of Ca and bioactivity [69].

Malavasi et al. [70] derived a mathematical relationship through a MD simulation that relates the Ca/P ratio in heterogeneous Ca-phosphate domains to the  $P_2O_5$  content in ternary  $SiO_2$ –CaO– $P_2O_5$  gel-glasses for fine-tuning the optimum amount of P to achieve the highest *in vitro* bioactivity. They found that the composition with optimal Ca/P ratio is 80SiO<sub>2</sub>–14.8CaO–5.2P<sub>2</sub>O<sub>5</sub> (mol-%), and bioactivity tests have confirmed their prediction [70]. This is indeed a very relevant result towards predicting useful glass properties.

More recently, Côté et al. [71] performed MD simulations to investigate how calcium interacts with silica during a sol–gel process, whose initial configuration includes  $Si(OH)_4$  monomers that are formed from the hydrolysis of the tetraethoxysilane (TEOS) precursors, during sol–gel processing of BGs. For this purpose, the atomistic evolutions of calcium-containing and Ca-free bioactive gel-glasses were compared using ReaxFF MD simulations. The ReaxFF class of force fields has proven to be very successful in modelling the chemical reactivity of a wide range of systems, rupture and formation of covalent chemical bonds in the course of the sol–gel process. The simulation results highlighted that calcium significantly accelerates the rate of poly-condensation leading to the formation of large, ramified silica clusters in 5 ns. It is believed that Ca induces nano segregation in calcium-rich and silica-rich regions and promotes the condensation reactions. Hence, unveiling the mechanism behind the incorporation of calcium in the early stages of the sol–gel process could guide further studies aimed at identifying complementary experimental conditions to produce gel-derived biomaterials with enhanced properties [71].

In addition to Na, Ca and P, whose structural roles in 45S5 and gel-derived  $SiO_2$ –CaO– $P_2O_5$  glasses have been revealed by solid-state NMR and MD simulations [72,73], the structure of silicate/phosphate BGs

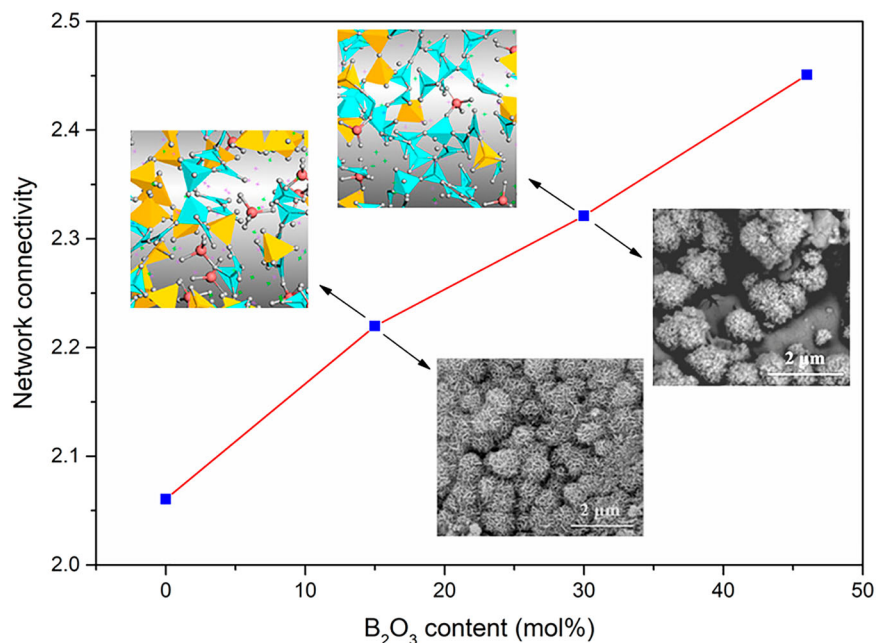


**Figure 4.** Correlation between the content of B<sub>2</sub>O<sub>3</sub>-substituted SiO<sub>2</sub> in 45S5 Bioglass<sup>®</sup>. The images show the formation of HAP *in vitro*, and the network connectivity by MD simulations (reproduced from the graphical abstract in Ref. [68] after permission from the American Chemical Society).

containing other elements and water [74], which impose important biological or structural changes, have been extensively investigated by MD simulations and, in some cases, compared to experimental data. These elements include cerium [75,76], magnesium [77], chlorine [78], fluorine [79–85], zinc [86–88], boron [89–92], strontium [93–95], gallium and aluminium [96], silver [97], copper [98,99], and lithium [100]. In most cases, MD simulations confirmed experimental observations of the structure determined by nuclear magnetic resonance (NMR), neutron scattering, and other types of experimental structural characterisation. For example, Figure 5 shows the local structure around cerium ions in cerium-doped bioactive phosphosilicate and silicate glasses revealed by X-ray absorption fine structure (XAFS) at the Ce K-edge, combined with CMD simulations. Cerium ions (Ce<sup>3+</sup> or Ce<sup>4+</sup>) are antibacterial and antioxidant agents; small quantities favour depolymerisation, dissolution and the antioxidant activity in silicate glasses. Conversely, the formation of cerium phosphate domains in phosphosilicate glasses is detrimental for both the solubility and catalytic activity [75,76].

Christie et al. [101], Côté et al. [102] and Eckert [103] demonstrated the successful use of high-energy X-ray and neutron scattering/diffraction methods, NMR, combined with classical/*ab initio*/CPMD/reactive MD simulations as components of a powerful strategy for the study of BGs. Overall, the combination of experimental and MD studies is very effective for systematically investigating the relationship between glass structure and bioactivity, as well as to understand the structural origin of several other properties, such as density, glass transition temperature, elastic modulus

and chemical durability of complex glass compositions. This integrated approach can be highly valuable for designing next-generation BGs. Finally, the biological responses to ions released from BGs and their structural roles revealed by MD simulations and experimental methods are summarised in Table 1. However, fine-tuning the dissolution rate of ion-doped BGs within the therapeutic range is still an open and challenging issue.

### Descriptors defining chemical degradation of BGs

The key challenges in biodegradation related to glass structure are the need to have experimental results covering the biodegradation of a broad range of suitable compositions and the task of devising structural descriptors by MD simulation, such as network connectivity, ion clustering, nano-segregation, and organisation in chain and ring nanostructures or other structural descriptors. For example, the first dissolution stage following implantation of Bioglass<sup>®</sup> in a physiological environment was simulated by Tilocca and Cormack [104,105] by CPMD simulations of the interface between the 45S5 Bioglass<sup>®</sup> and liquid water. The investigation of a 40 ps CPMD trajectory highlighted the potential mechanism of Na<sup>+</sup>/H<sup>+</sup> exchange in the initial stages of the bioactivity mechanism, previously envisaged by Hench [104,105]. Zeitler and Cormack [106] then simulated the bulk structure of 45S5 glasses to elucidate the second reaction step in the proposed mechanism of bioactivity, which is the dissolution of bonds between oxygen and the network forming cations of silicon and phosphorus. MD simulations showed that the dissolution energy varies considerably



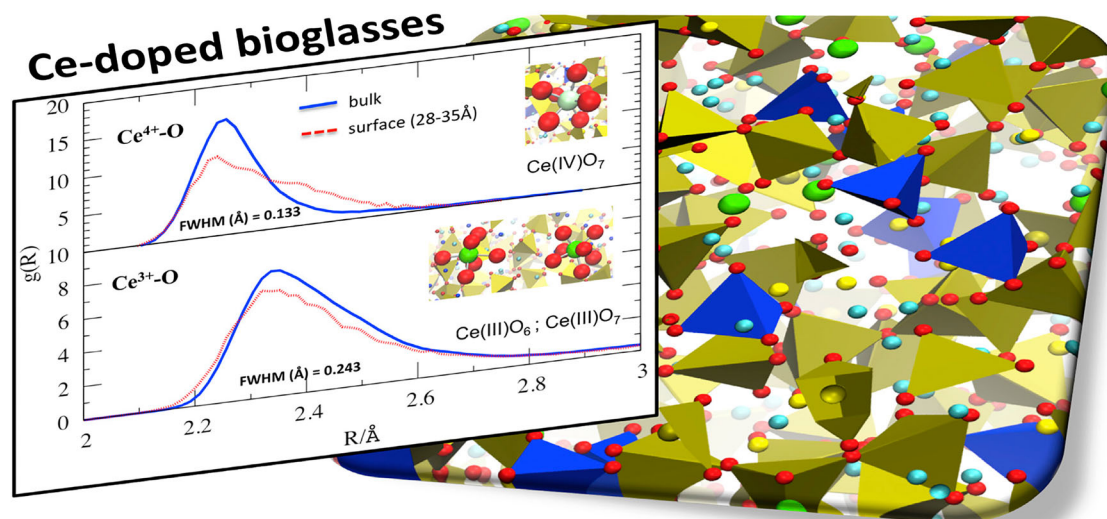


**Figure 5.** Pair distribution functions,  $g(R)$ , for Ce–O pairs in silicate and phosphosilicate BGs. The figure on the LHS shows the values of full width at half maximum (FWHM) for the peaks in the XAFS spectra at the Ce K-edge for phosphosilicate (top) and silicate (bottom) glasses. The insets illustrate the typical oxygen arrangements around the Ce ions obtained by MD simulations [75]. The image on the RHS is the simulated structure of phosphosilicate glass by MD.

depending on the nature and environment of the Si–O–Si bond being broken. However, no apparent correlation with bioactivity was observed, suggesting that, although the network disruption is a necessary process, it is not rate-determining [105,106]. In a related article, Tilocca, Cormack, and De Leeuw [107] simulated the changes in the network connectivity, coordination environment, and ion aggregation with the silica content to provide new insight into the physicochemical behaviour of these materials. The experimentally observed transition from highly bioactive to inert compositions was identified through modelling by a marked increase in the network connectivity of the silicate and by an increasing fraction of phosphate groups involved in the network. Their analysis highlighted a possible correlation between the loss of bioactivity and a significant aggregation of  $\text{Ca}^{2+}$  and  $\text{PO}_4^{3-}$  ions, which leads to calcium-phosphate-rich regions for a bio-inactive composition containing 65%  $\text{SiO}_2$  [107]. However, this effect could be counterbalanced by the simultaneous increase in the amount of free orthophosphate groups ( $\text{PO}_4$  groups,  $\text{Q}^0$ ), which released quickly, enhancing the bioactivity. The strong tendency for orthophosphate formation also leads to a separation of silicate-rich and phosphate-rich regions (a network of pyro- and polyphosphate groups,  $\text{Q}^1$  to  $\text{Q}^4$ ) for compositions having a high content of phosphorus (12 mol-%). Although this phase separation could reduce bioactivity, overall the favourable balance between an increase in orthophosphate content should result in a positive effect of partial substitution of Si by P on the glass bioactivity [108].

The detailed reaction of BGs with water has been simulated by Tilocca and Cormack, [109] and [110], to investigate the surface of a highly bioactive Na +

Ca phosphosilicate glass. Figure 6 shows an example for the interaction of water with an active site on a silicate glass surface. Spontaneous water dissociation was observed on the glass surface, represented by three-coordinated Si atoms associated with proton acceptors, such as nonbridging oxygens. Additional adsorption sites were found to be related to the Na/Ca modifiers, which are involved in the glass dissolution and provide favourable pathways to allow water to penetrate the surface. Small silica rings, 2- or 3-membered (2M or 3M) rings, were found to be stable features on the surface, although there was a possible configuration allowing their opening upon water dissociation. The minimum energy barriers for 2M ring-opening mechanisms, obtained using String Method Car-Parrinello calculations, revealed that an energy barrier suppresses the opening of small rings. The simulation showed that small closed rings that are hydroxylated after immersion in an aqueous environment assist with the nucleation of Ca and P ions on the surface, which was previously proposed to understand the initial stages of the bioactive mechanism [109]. In another study, they modelled the surface of a bioactive (46.1 $\text{SiO}_2$ –24.35 $\text{Na}_2\text{O}$ –26.9 $\text{CaO}$ –2.57 $\text{P}_2\text{O}_5$  in mol-%) and a bio-inactive (66.9 $\text{SiO}_2$ –14.47 $\text{Na}_2\text{O}$ –15.98 $\text{CaO}$ –2.63 $\text{P}_2\text{O}_5$  in mol-%) glass composition in contact with water. The simulations highlighted the important role of network fragmentation and sodium enrichment of the surface in controlling the rapid hydrolysis and release of silica fragments in solution, characteristic of highly bioactive compositions. On the other hand, no correlation was established between the surface density of small (2- and 3-membered) rings and bioactivity, thus signifying that additional factors must be considered to understand more fully the role of these

**Table 1.** Biological responses to ions released from BGs and their structural roles revealed by MD simulations and experimental techniques.

Ion	Biological response <i>in vivo/in vitro</i> [26–28]	Structural roles revealed by MD simulations and experimental techniques
Si	<ul style="list-style-type: none"> <li>Essential for metabolic processes, formation and calcification of bone tissue.</li> <li>Dietary intake of Si increases bone mineral density.</li> <li>Aqueous Si induces HAp precipitation.</li> <li>Si(OH)<sub>4</sub> stimulates collagen formation and osteoblastic differentiation.</li> </ul>	455S Bioglass® contains chains and rings of Q <sup>2</sup> (67.2%) SiO <sub>4</sub> tetrahedra cross-linked with Q <sup>3</sup> (22.3%) species and terminated by a smaller quantity of Q <sup>1</sup> (10.1%) species [64].
Ca	<ul style="list-style-type: none"> <li>Favours osteoblast proliferation, differentiation and extracellular matrix mineralisation.</li> <li>Activates Ca-sensing receptors in osteoblast cells, increases the expression of growth factors.</li> </ul>	A modifier which surrounds NBOs [64].
P	<ul style="list-style-type: none"> <li>Stimulates expression of matrix la protein, a key regulator in bone formation.</li> </ul>	Isolated orthophosphate units can form, when P <sub>2</sub> O <sub>5</sub> content is ~1–6 mol-%, building nano-domains with sodium and calcium cations [64–66].
B	<ul style="list-style-type: none"> <li>Potential stimulating agent for bone tissue engineering.</li> <li>Dietary boron stimulates bone formation.</li> </ul>	Two species of boron ( <sup>3</sup> B and <sup>4</sup> B) have been observed. Increases the overall network connectivity in 455S Bioglass® [68]. Changing pH value tends to release of boric acid into the solution. Also, the inability to form silica gel due to fast dissolution could be the main reason for the slower rate of HAp formation with higher boron oxide in the glass composition (Figure 4) [89].
Zn	<ul style="list-style-type: none"> <li>Shows anti-inflammatory effect and stimulates bone formation by activation protein synthesis in osteoblasts.</li> <li>Increases ATPase activity, regulates transcription of osteoblastic differentiation genes, osteopontin, and osteocalcin.</li> </ul>	It plays an intermediate role. The majority of Zn ions (over 80%) are 4-coordinated and connect with the SiO <sub>4</sub> tetrahedra. Also, 5-coordinated Zn ions and oxygen were found in the glasses [86].
Mg	<ul style="list-style-type: none"> <li>Stimulates new bone formation.</li> </ul>	Mg in 455S Bioglass® is coordinated by 5 NBOs of different PO <sub>4</sub> or SiO <sub>4</sub> tetrahedra leading to large rings in the structures. Mg is almost absent in Ca–Na-phosphate rich regions [77].
Sr	<ul style="list-style-type: none"> <li>Increases bone cell adhesion and stability.</li> <li>Shows beneficial effects on bone cells and bone formation <i>in vivo</i>.</li> <li>Promising agent for treating osteoporosis.</li> </ul>	Have a slightly higher coordination number (CN) and longer cation–O bond distance than Ca. In 5 mol-% SrO containing 455S Bioglass®, CN ≈ 7.0 and the Sr–O bond length is ~2.56 Å. The diffusion energy barrier for Sr is ~0.80 eV [93–95].
Ce	<ul style="list-style-type: none"> <li>Promotion of angiogenesis.</li> <li>Antibacterial.</li> <li>Scavenging superoxide radicals.</li> <li>Enhances the osteoblastic differentiation of human mesenchymal stem cells and the production of collagen.</li> </ul>	Increase depolymerisation, and dissolution of silicate BGs. Conversely, the formation of cerium phosphate domains in phosphosilicate BGs is detrimental for both the solubility and ion activity [75,76].
F	<ul style="list-style-type: none"> <li>Antibacterial.</li> <li>Inhibits the formation of alveolar cavities.</li> <li>Provides higher acidic resistance of enamel by substituting OH sites in dental apatite.</li> <li>Has stimulating effects on osteoblast cells when applied at moderate concentrations.</li> <li>Results in slightly pH raise and favoured formation of fluorapatite (FAP).</li> </ul>	Is usually present as isolated fluoride ions in silicate BGs, which form strong ionic bonds to the network modifiers (CN ~4) rather than bonding to the silicate network (no Si–F bonds), causing structural nano-heterogeneities [79,82,83,85]. In contrast, it induces re-polymerisation in the phosphate BGs by stripping the network modifying cations from the glass network [80] and forming F–P bonds, without inducing inhomogeneities [81].
Cl	<ul style="list-style-type: none"> <li>Cl-containing is more soluble than F-containing BGs and will convert completely to HAp in the presence of water, enhancing bone formation and suitable for making resorbable bone substitutes.</li> </ul>	No Si–Cl and P–Cl bonds detected. Chlorine anions are present as Cl–Ca. In the mixed-fluoride/chloride-containing glasses, fluorine tends to surround phosphate, whereas chloride moves toward the silicate network [78].
Ga	<ul style="list-style-type: none"> <li>Antibacterial effects.</li> </ul>	Predominantly is in a 4-fold coordination environment, small amounts of 5- and 6-fold coordinated atoms have been detected, suggesting its possible intermediate role in phosphosilicate BGs and it does not form segregated regions [96].
Ag	<ul style="list-style-type: none"> <li>Antibacterial and anti-inflammatory effects.</li> </ul>	Bind to the phosphate chains and clustering happens at low concentrations of silver [97].
Cu	<ul style="list-style-type: none"> <li>Angiogenesis and antibacterial/antimicrobial effects.</li> </ul>	Cu <sup>+</sup> and Cu <sup>2+</sup> ions form P–O ... Cu linkages in phosphate glasses that could contribute to ion diffusion and release [98].
Li	<ul style="list-style-type: none"> <li>Stimulate osteoblast cell activity and angiogenesis.</li> </ul>	Fast moving modifier ion which should be released within the therapeutic range (< 8.3 ppm). Each Q <sup>3</sup> unit is surrounded by approximately three lithium ions at an average distance of 320 pm, whereas the Q <sup>4</sup> units are much more remote from lithium [100,103].

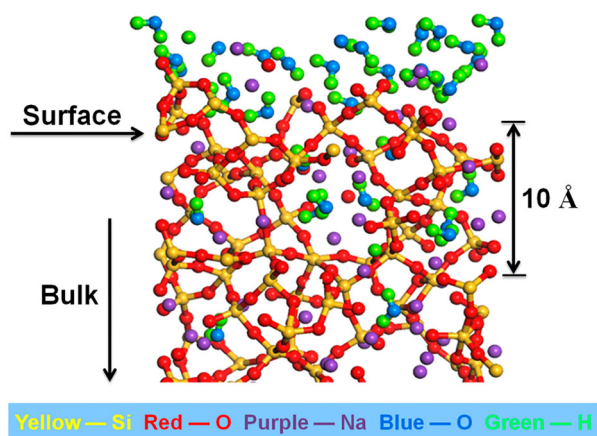


**Figure 6.** Water adsorption on the surface of  $\text{Na}_2\text{O-SiO}_2$  glass simulated by MD. Si, O, and Na in the glass are represented as yellow, red, and purple balls, respectively. Hydrogen and oxygen of water are shown by green and blue balls, respectively (modified with permission from Ref. [112]).

sites in the mechanism of calcium phosphate precipitation on the glass surface [111].

In addition to phosphosilicate glasses, which are archetypal BGs, bioactive phosphate-based glasses have numerous potential biomedical applications due to the chemical reactions/degradations they undergo with their surroundings when implanted into the body. The dissolution rate of these degradable glasses in physiological conditions is an important factor for these applications to ensure the desirable rate of drug delivery or nutrients to the body. Christie et al. [113] provided, for the first time, an atomistic explanation of the fact that the substitution of  $\text{Na}_2\text{O}$  by  $\text{CaO}$  in these glasses retards the dissolution rate. In this work, MD simulations of ternary  $\text{P}_2\text{O}_5\text{-CaO-Na}_2\text{O}$  glasses revealed their structural properties at the atomic level that enhanced the durability as more Ca is added. Calcium first binds to more fragments of the phosphate glass network than Na. Second, it ties together more  $\text{PO}_4$  tetrahedra than Na. Also, Ca has a lower concentration of intratetrahedral phosphate bonding than Na. This behaviour is due to the calcium ion's higher charge and field strength. These results could help to open a path to precise control and optimisation of the degradation rate of phosphate BGs for specific applications [113].

Tilocca, Christie, and Malik [114–116] identified new structural descriptors that influence the solubility and, therefore, the performances of yttrium-doped glasses used as radioisotope vectors for *in situ* radiotherapy, an application which also depends on the glass durability. Glasses used for this purpose do not need to be bioactive, but they must be biocompatible and radioactive to kill malignant tumours. Yttrium-doped glasses have been successfully used clinically for 25 years [39]. These glasses containing yttrium isotope ( $^{90}\text{Y}$ ) are made by neutron activation as the last step in the manufacturing process, only a few hours

before clinical application [117]. The structural descriptor for  $\text{SiO}_2\text{-P}_2\text{O}_5\text{-Na}_2\text{O-CaO-Y}_2\text{O}_3$  glass identified by MD simulation was non-covalent cross-links between separate portions of the silicate network, bridged by a modifier cation, which was yttrium in this case (Figure 7). They found that higher-yttria compositions with constant network connectivity are characterised by a less dense but stronger network of NBO-Y-NBO cross-links, as well as reduced yttrium clustering. Their simulation thus showed that it should be possible to produce  $^{90}\text{Y}$ -doped BGs with sufficient biological activity to support the growth of new tissues and capable of delivering higher radiation doses through higher yttria content. The unwanted dissolution of harmful amounts of radioactive yttrium should be limited by the strong linkage of yttrium with non-bridging oxygens, which prevents an overly rapid degradation of the glass network [39,114–116].

### MD simulation of ion migration in BGs

MD simulations have also investigated the migration of modifier ions in silicate and phosphate BGs. It is well-known that the open structure of 45S5 Bioglass<sup>®</sup> leads to fast ion migration, which is slower in the denser network of conventional high silica-containing non-bioactive (inert) glasses [118]. It is known that ion migration in BGs is very slow at room temperature, requiring prohibitively long trajectories to obtain a reasonably accurate sampling of the diffusion process. Fortunately, most MD studies of diffusion in glasses of biomedical interest to date have adopted an effective strategy to handle this problem, wherein simulations are run at a high temperature, but still below the glass transition [118–120]. It is shown that the modifier ions move in a static silicate/phosphate network, whose average configuration and energy landscape match those of the stable configuration at room temperature, so that the description of the diffusive phenomenon at high temperatures is still representative of realistic conditions [118–120]. Another difficulty is the possible inadequacy of the interatomic potentials employed in classical MD runs. A potential that provides a good picture of the glass structure does not necessarily perform as well in reproducing dynamic processes. A more rigorous solution would be represented by parameter-free *ab initio* MD (AIMD) approaches [121]. The higher computational demands of this approach, however, limit the AIMD trajectory length to below the nanosecond range, with the consequence that an investigation of the migration of sluggish cations is complicated, even with the high-temperature strategy described above [121]. MD simulations have been employed to trace ion migration in the structure of 45S5 glass. Modifier ions travel through vacant transient sites created by temporary displacements of another Na or Ca cation (Figure 8) [118]. The formation of these

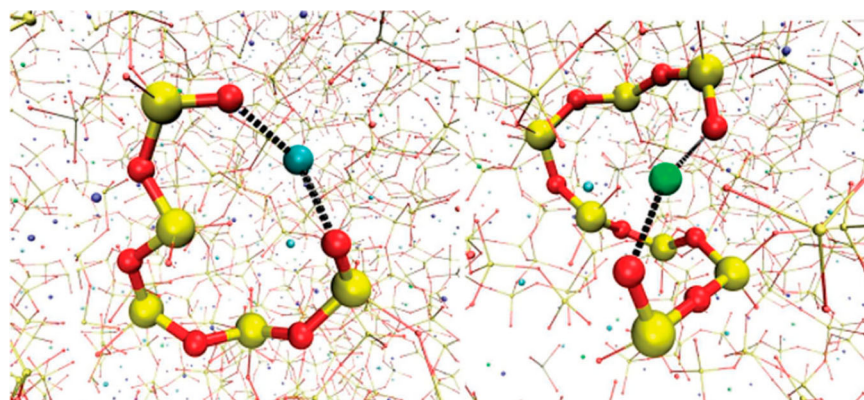


**Figure 7.** Identifying modifier ions (the sphere at the centre of the loop, left: Ca, right: Y) in the structures of a Y-doped glass. These ions crosslink two tetrahedra belonging to the same chain fragment. They are holding the  $O_3SiO-(SiO_2)_n-O_3SiO_3$  unit in place and thus increasing the network durability. Adapted from Ref. [115] with permission from RSC.

temporary sites, even if still possible, would not be as favourable in the more rigid network of a higher-silica glass [122]. AIMD has been employed to characterise sodium migration in 45S5 Bioglass® (Figure 8), but not enough calcium migration steps were observed during the simulation time to provide an equally clear picture of the (slower) diffusion of Ca [118]. Therefore, a more rigorous approach for tackling the timescale problem affecting MD simulations of ion migration in glasses, which experiences complex energy landscapes encountered by ions migrating in multicomponent BGs, is a required *challenge for the future* [51]. An effort made by Tilocca to model, through MD simulations, ion migration in two fluoride-containing BGs of significantly different durability [123]. The structural features of BGs could not (alone) explain their very complex chemical degradation, then the analysis of ion diffusion helped to correlate the glass durability determined experimentally and the activation barrier extracted from the simulations. This clarified the source of the different solubility and suggests ‘dynamical’ descriptors of bioactivity as a key tool to predict the degradation of biomaterials, in some cases more effectively than with the current structural descriptors [123]. Moreover, this study suggested the possibility of screening some potentially interesting compositions by investigating experimental ionic conductivities of BGs as an alternative or complementary tool to the customary ion release experiments in simulated body fluid [123,124].

### MD simulation of nano-BGs

MD simulations can also model crystalline and glassy nanoparticles (NPs). In an isolated 5–15 nm particle of a BG, there are  $10^4$ – $10^5$  atoms, which is an achievable size for classical MD [125,126]. Tilocca [125] has simulated a spherical nanoparticle of 45S5 Bioglass® with a 6-nm diameter to investigate the main structural characteristics induced by the reduced size, which

could play an essential role in the enhanced bioreactivity of these particles, in addition to their higher surface area. A suitable computational procedure involves fast quenching a liquid mixture constrained within an isolated sphere of the desired size, roughly replicating the flame spray synthesis used to prepare small BG nanoparticles [126]. MD simulations confirmed the idea that the most relevant influences of the reduced size are a further reduction in the connectivity on the surface of nanoparticles, together with an increase in the number of three-membered rings and a higher  $Na^+/Ca^{2+}$  ratio near the surface [125]. Moreover, the mobility of the modifiers and the density of 3-membered silicate rings – key characteristics to sustain rapid dissolution and bone-bonding processes at the surface – are also enhanced at the nanoparticle surface compared to larger samples [125].

Furthermore, Pedone et al. [127] used MD simulations to study two glass nanoparticles with compositions of  $25Na_2O-25CaO-50SiO_2$  (mol-%) (Ce-K NP) and  $46.1SiO_2-24.4Na_2O-26.9CaO-2.6P_2O_5$  (mol-%) (Ce-BG NP) doped with 3.6 mol-% of  $CeO_2$  to explain the effect of cerium on their enhanced antioxidant effect. Their models (see snapshots of the final structures in Figure 9) showed that the different antioxidant activity of the two glasses is related to the different  $Ce^{3+}/Ce^{4+}$  ratios exposed at the surface. The ratio was  $\sim 3.5$  and 13 in bulk and at the surface of the Ce-BG NP, and 1.0 and 2.1 for the Ce-K NPs, respectively. A higher  $Ce^{3+}/Ce^{4+}$  ratio reduced antioxidant properties. Moreover, the simulations identified reduced network connectivity and enhanced  $Na^+/Ca^{2+}$  ratio on the nanoparticle surface. Na, Ca and Ce sites in the proximity to the surface are under-coordinated, leading to quick reaction with water in physiological environments, thus accelerating the glass biodegradation [127–129].

The challenge in MD simulations of nanoparticles is to take into account the perturbation induced by the physiological fluids that come into contact with the particle. Thus, modelling of the interface between the

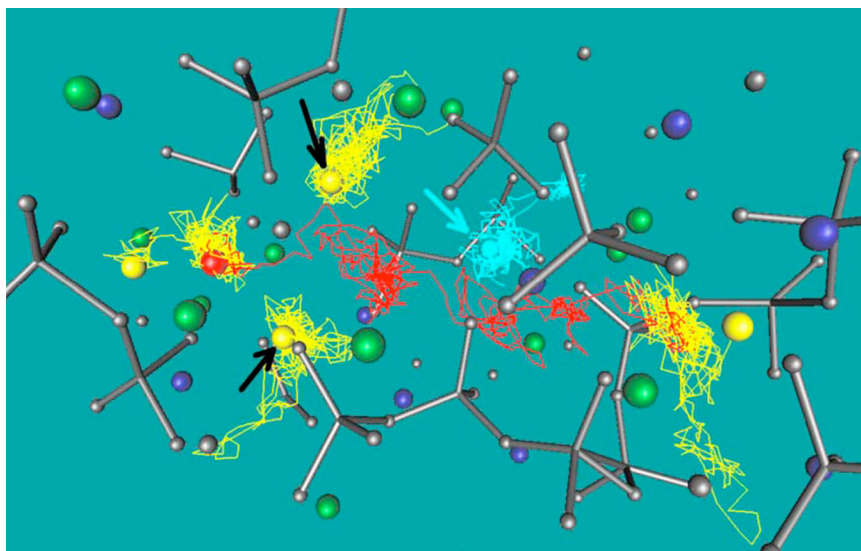


**Figure 8.** 3D traces of the trajectory of Na and Ca ions in 45S5 Bioglass<sup>®</sup>, illustrating the migration of an individual Na<sup>+</sup> ion (red) and the correlated displacements of several other atoms (Na atoms, yellow and Ca, cyan). Green spheres are phosphorus, and the silicate network is represented as grey ball and stick. Reprinted with permission from Ref. [118], American Institute of Physics.

nanoparticle and an aqueous medium is quite difficult, as well as assessing the effects of this interaction on the properties of the system. It demands accurate force fields to simulate the extra interactions at the biomaterial interface (the considerable size of the models prevents the straightforward use of AIMD approaches in this case) and longer simulation times compared to the dry cases and largest NPs [51].

### Big data and ML

A future is envisaged in which artificial intelligence (AI) methods as part of ML strategies will significantly accelerate the design, discovery, synthesis, characterisation, and application of materials [130,131]. Computational simulations utilise physical-chemistry-based principles, statistical mechanics, and numerical methods to extract insights into the *structure-*

*chemistry-property* relationships of materials. On the other hand, ML applications in materials science build empirical models using algorithms that iteratively learn from data to find hidden relationships and build predictive models. ML involves several steps: raw data collection, data cleaning, training and model building, and model testing and evaluation [130–133]. Regardless of the problem under study, a precondition for ML is the existence of a collection of clean, reliable, and curated data relevant to the particular problem under investigation. Often, the greatest effort is involved in the creation and pruning of the data set. In the ML approach, the target property can be a continuous quantity (e.g. hardness, density,  $T_g$ , liquidus temperature, etc.), i.e. regression problems, or discrete targets (e.g. crystal structure, specific structural descriptors, etc.), which are referred to as classification problems. Throughout the ML procedure, it should be

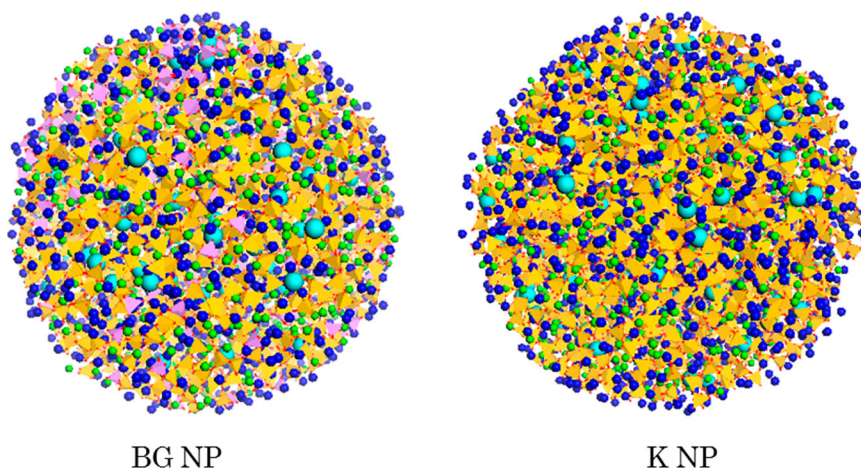


**Figure 9.** Snapshots of the final structures of the nanoparticles investigated by Pedone et al. after the MD simulation. Yellow and violet tetrahedra are silicate and phosphate units, respectively, whereas the blue spheres are Na, Ce ions are cyan, and Ca are the green spheres [127].

possible to predict unseen data ensuring that a trained model based on the original dataset can handle new cases. Figure 10 summarises the general process of ML in study BGs. Besides this graphical description, interested readers can refer to recent comprehensive papers addressing the principles, applications, and perspectives of ML in materials science [130–133]. However, the materials science community is just beginning to explore and use the plethora of available tools and algorithms to mine and learn from existing data. ML should be viewed as the combination of the organised creation of initial datasets, the learning and training steps, and the necessary subsequent steps of progressive and targeted infusion of new data [130–133].

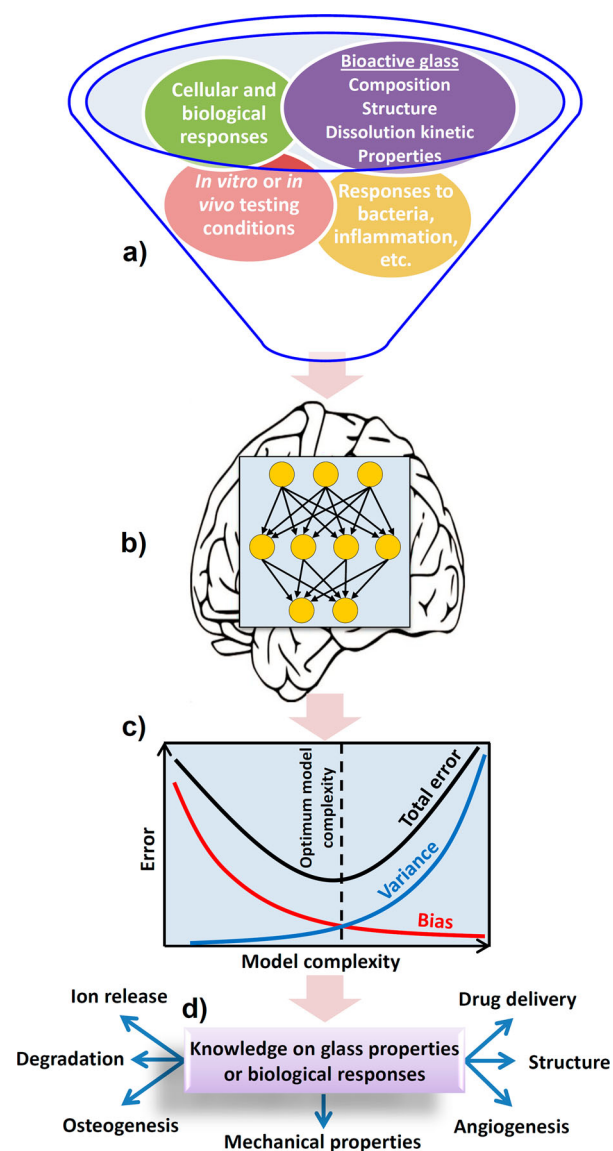


**Figure 10.** Schematic of the general machine learning processes in the study of bioactive glasses. (a) data analysis and cleaning, (b) model building, e.g. through artificial neural networks, including learning methods, regression, classification, clustering, probability, estimation and optimisation, (c) model evaluation, e.g. by minimising bias and variance, and finally (d) obtaining knowledge on properties of BGs or biological responses.

In the design of biomaterials, combinatorial and computational methods could be used to transition the traditional (empirical and semi-empirical) mode of materials discovery into an intelligent (physics-based and AI-driven) mode of exploration and discovery. As an example, biopolymer libraries are an excellent means to explore a wide range of polymer compositions efficiently and in a cost-effective manner. Computationally modelled structures are then used to make predictions of polymer properties, enabling a rational approach to choose a subset of the resulting virtual polymers for laboratory synthesis and examination [134,135].

In the field of bioactive oxide glasses (which includes the most important families of BGs), only two published articles have tested the applicability of ML approaches for predicting chemical solubility [136], and bactericidal effect [137]. Brauer et al. [136] experimentally classified the solubility of degradable phosphate BGs of  $P_2O_5$ -CaO-MgO- $Na_2O$ - $TiO_2$  in water for 60 min at 98°C to obtain a small dataset for ANN modelling. A dataset of 30 glass compositions versus pH variations and dissolved  $P_2O_5$  in  $mg\ L^{-1}$  was obtained. Through the increase of the  $P_2O_5$  content in the glass composition, the glasses showed a higher solubility and yielded lower pH values in aqueous solution, which is due to the underlying structural changes, since long phosphate chains are more affected by hydration than smaller chains. These changes in the glass structure were first determined by  $^{31}P$  MAS-NMR experiments [136]. Increasing  $Na_2O$  concentrations at the expense of CaO or MgO also increased the glass solubility by disrupting ionic cross-links between chains. By contrast, the addition of  $TiO_2$  rendered the glasses more stable towards dissolution by cross-linking smaller phosphate groups. The authors could not find a relationship between glass composition and solubility using classical regression data analysis, but a preliminary ANN analysis demonstrated, for the first time, that AI is indeed a valuable tool for modelling the solubility of BGs [136].

In another study, Echezarreta-López and Landin [137] found relationships between the antibacterial behaviour of BGs and glass composition using a trained neural network. We summarise their method to show this first attempt of using fuzzy logic in combination with ANN to model this very important biological property of BGs. The authors chose several BGs from 10 published articles from 2000 to 2010. The antimicrobial activity studies probe the antibacterial effect of BGs by culturing them with selected bacteria species in specific culture media. After a preset time of cultivation, the pH was measured, and a certain volume of the culture was transferred, cultivated on a new media and the bacterial growth index (GI) was estimated. Two models were designed. In a first model (Figure 11), 21 variable inputs were selected,

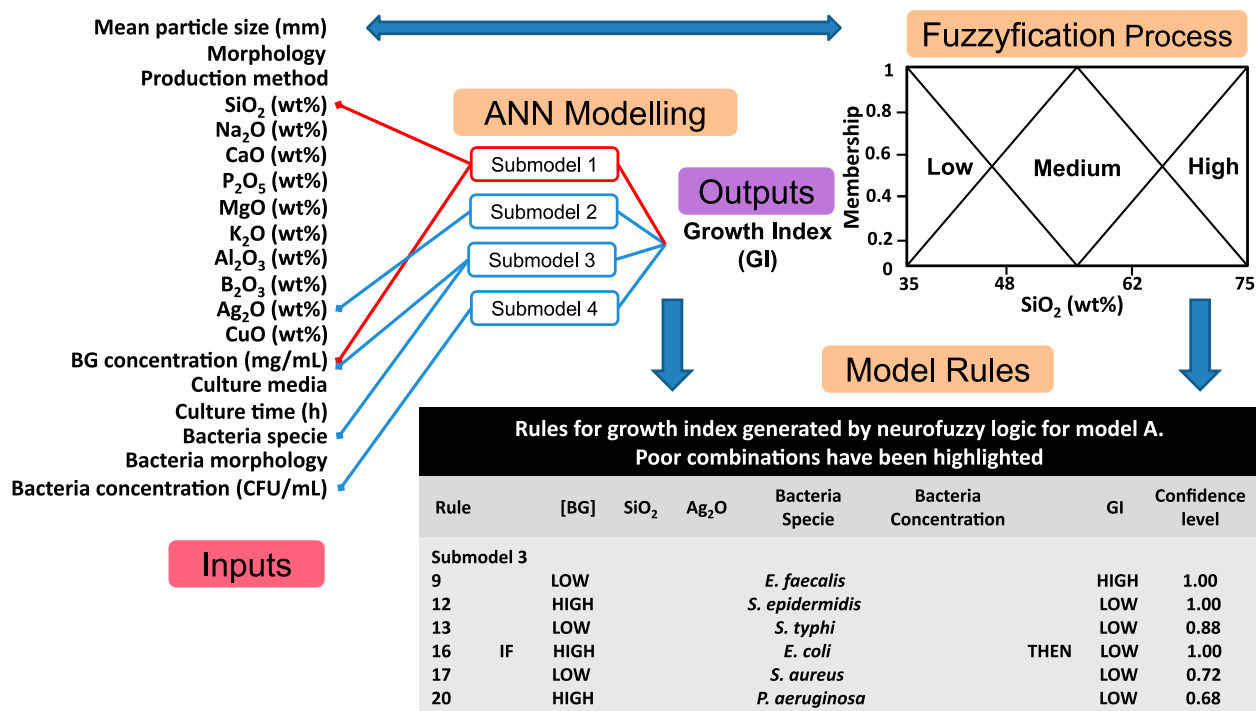


**Figure 11.** Combination of a machine learning approach, ANN, and Fuzzyfication for predicting antibacterial properties of BGs (reproduced from the graphical abstract of Ref. [137], with permission from Elsevier).

which reduced the dataset from 531 to 348 and classified it into three input groups: BG characteristics, bacterial characteristics, and experimental microbiological conditions. Among the BG characteristics, the production method, BG composition regarding concentration of SiO<sub>2</sub>, CaO, Na<sub>2</sub>O, P<sub>2</sub>O<sub>5</sub>, MgO, K<sub>2</sub>O, Al<sub>2</sub>O<sub>3</sub>, B<sub>2</sub>O<sub>3</sub>, Ag<sub>2</sub>O, CuO (wt.%), mean particle size ( $\mu\text{m}$ ), morphology: nanoparticles, powder, particles and fibres, and BG concentration ( $\text{mg mL}^{-1}$ ) were selected. For every experiment, the bacterial characteristics considered were: microorganism species (including *Staphylococcus aureus*, *Staphylococcus epidermidis*, *Enterococcus faecalis*, *Escherichia coli*, *Pseudomonas aeruginosa*, and *Salmonella typhi*) and morphology (bacillus or coccus). Bacteria were grown aerobically in different microbiological experimental conditions registered as bacterial concentration ( $\text{CFU mL}^{-1}$ ), culture time (h) and culture media categorised in two groups named as buffered solutions (when used, simulated buffered fluid, phosphate buffered saline or solution saline) and nutrient solution (when used, Tryptone Soy broth, Lysogeny broth, Mueller Hinton broth or nutrient broth). Also, co-culture time and co-culture media (using the same categorisation as previously noted) were registered. In another model, final pH values were also included as an additional input. This approach reduced the number of facts to 129. For both models, the output recorded was the GI, measured as a function of the number of survival bacteria colonies. The absence of growth ( $\text{GI} = 0$ ) indicates a bactericidal effect [137].

Very sparse and moderate values of GI ( $\text{GI} = 1$  between 0 and 5 colonies,  $\text{GI} = 2$  between 5 and 50,

and  $\text{GI} = 3$  between 50 and 300 colonies, respectively) indicated a moderate growth. The GI of 4 ( $>300$  colonies) indicates no effect. A database with the inputs and outputs from the various sources was compiled. Then the dataset analysed by neuro-fuzzy logic technology. This study provided the first use of ANN and data analysis on the variability in antibacterial behaviour reported by different authors to obtain general conclusions about critical parameters of BGs to be considered to combat some of the most common skin and implant surgery pathogens [137].

This study shows that AI technology allows a novel and integrated analysis of the results from the literature on antibacterial activity of BGs. Neurofuzzy logic was able to model a database on BGs, to determine the critical variables for BG antibacterial activity and to present conclusions. While it is believed that the antibacterial property of BGs is mainly elicited by incorporation of therapeutic metallic ions such as silver ( $\text{Ag}^+$ ), zinc ( $\text{Zn}^{2+}$ ), copper ( $\text{Cu}^+$  and  $\text{Cu}^{2+}$ ), cerium ( $\text{Ce}^{3+}$  and  $\text{Ce}^{4+}$ ), and gallium ( $\text{Ga}^{3+}$ ) into their structure [26,31], the resulting ANN model revealed that antibacterial activity is also affected by the release of alkaline ions to the medium with a resulting increase of pH [137]. Important variations in BG antibacterial activity on different species of bacteria are mainly linked to the composition of the BG and, in particular, to their content of calcium ions. The differences found in the susceptibility of different bacterial species concerning this chemical entity should lead to addressing the study of antibacterial activity of BGs on a wide selection of bacterial flora to the possible impact on the pathology or

the process in which its use will be involved. The microbiological conditions studied (culture and co-culture media and time) did not have a significant impact on the results of the studies of BGs antimicrobial activity [137].

In another ML endeavour, which was focused on process variables, Yilmaz et al. [138] modelled the diameter of the bioactive electrospun fibres by ANNs. Since fibre diameter depends on various parameters (process variables, solution, and environmental parameters), they used a multilayer perceptron (MLP) strategy for predicting the average diameter of electrospun gelatin/bioactive fibre glasses (Gt/BGs) mixtures. These nano-fibrous materials are very promising for assembling scaffolds for tissue engineering enabling to deliver drugs, growth factors, and stem cells. The experimental results, which report one solution parameter (BG content) and two process parameters (tip to collector distance and solution flow rate) were used. The dataset was built based on the parameters of the 15 Gt/BGs samples were employed for the training step of the model and furthermore, the remaining 4 samples were used to evaluate the accuracy of the model. The average percentage error between the predicted average fibre diameters and experimental values was 3.3%. The authors claimed that the resulting model could accurately predict the average fibre diameter of electrospun Gt/BG without requiring any complicated or sophisticated knowledge of the mathematical and physical background [138].

In the field of BGs, to the best of our knowledge, only the three abovementioned studies have used ML approaches. However, the number of data points used in these studies to train and test the resulting algorithms were very small (31, 15 and 531 facts, respectively), which is not recommended [139] for building ANN models due to the strong possibility of overfitting. Nevertheless, they reported that the used ANNs reasonably predicted the chemical solubility, antibacterial properties, and fibre diameter of the investigated materials.

As the amount of data available in the field of BGs science is already impressive and increasing at a rapid pace, big data analysis will certainly help to make them more uniform, discoverable, interpretable, and usable in ML approaches. We could find only one such research article published by Farano et al. [140]. They comprehensively reviewed the current findings on the effects of sol-gel-derived BGs on dental stem cells for dental and periodontal regeneration. Their study discusses and analyses reported data related to antibacterial properties. The research was conducted by considering the Preferred Reporting Items for Systematic Reviews and the Meta-Analyses (PRISMA) statement. It covered a period of five years (from January 2012 to August 2017), and the relevant studies were identified based on certain inclusion or

exclusion criteria. A total of 52 publications were selected from 244 initial returns. This systematic selection and study revealed that only 13 of the 52 articles proved both the ability of BGs to differentiate dental cells, at the genetic level and their capability to trigger cell-mediated mineralisation. But only 6 of these articles showed the antibacterial properties of the glasses. This study revealed that sol-gel BGs are non-toxic, can stimulate cell proliferation and differentiation at a genetic level, and can sustain the bacterial population under control. Moreover, a standard methodology and suitable material were suggested [140]. For example, a double doped sol-gel glass, with Sr and Ag (for instance), in association with a polymer, to make scaffolds (e.g. using electrospinning), could represent a preferred approach for novel products in dental tissue engineering.

## Perspectives

In the previous sections, we observed that only a few dozen MD simulations and a handful of ML studies have contributed to the modelling of BGs. It is quite clear that the development of new BGs for commercialisation is now only being conducted empirically, based on the accumulated knowledge and experience of the glass scientists, using a guided trial-and-error approach. This process is very expensive and time-consuming. As we have emphasised throughout this article, it is now time to move away from this 'cook and look' method to a new era of modelling and predicting compositions that might lead to novel glasses having unique, useful combinations of properties. To meet this need for substantial acceleration in the advancement of BGs, more sophisticated and complementary approaches must be developed and employed to enable faster, cheaper, and better R&D on new glass compositions for improved applications. One of us [9] has recently addressed different approaches for designing new glasses through the mathematical optimisation of composition-dependent glass property modelling. The models are based on combining (known) physical insights regarding glass composition-property and data-driven approaches, such as ML techniques. This combination of physical and empirical modelling approaches may help us to decode the 'glass genome.' However, successful modelling of product-facing properties is only half of the story. Ensuring that the discovered new glasses can be processable at a scale required to meet customer demands is *another challenge*. This must be achieved while minimising defects, such as inhomogeneities, unmelted batch materials, devitrification, gaseous inclusions or forming defects. Some important manufacturing-related properties include *viscosity, liquidus temperature, glass-forming ability, and batch cost* [9]. Unfortunately, these attributes have been only once



addressed by Fu et al. for the case of well-researched 45S5 and 13-93 BGs [141]. The properties of these two glasses including strain, annealing, and softening points, thermal expansion, density, and liquidus temperature were characterised. Both glasses exhibited a much lower liquidus viscosity than that of common soda-lime silica glass, suggesting a significant challenge for melting and forming of these BGs in a continuous-unit melting system.

Here we showed the capabilities and reliability of MD simulations, three cases of ML and a single meta-analysis research. Other promising modelling approaches, such as DFT, TCT, evolutionary algorithms, and Monte Carlo simulation, should be encouraged. Below, we briefly introduce some promising approaches (already applied in the field of other glasses) that might be employed to model BGs. Then, we argue that ML is a promising method to successfully model/predict more complex multicomponent compositions and biological responses.

### Physics-based modelling

Experimental data-driven models do not assume anything about the underlying physics governing material properties. However, incorporating known physics into the models broaden their applicability and extrapolation. Glassy materials are well-known to pose significant challenges based on their three ‘non’s, viz., glasses are noncrystalline, nonequilibrium, and nonergodic materials [4]. This means that standard equilibrium thermodynamic and statistical mechanical approaches cannot be used to capture the intricacies of the glassy state [142–149].

Mauro and Smedskjaer have proposed and reviewed new modelling approaches to address the challenges posed by glass-forming systems [149]. At the most fundamental level, the physics of glassy systems can be described using the framework of continuously broken ergodicity [150] and the energy landscape approach [151], which may be recast in terms of either an enthalpy landscape [152] or free energy landscape [153], depending on what is appropriate for the problem under study. The description of continuously broken ergodicity can capture the continuous vitrification of glass-forming liquids as they are cooled into the rigid glassy state and the continuous relaxation process as the glasses spontaneously approach the supercooled liquid state [150]. The energy landscape approach now enables a realistic calculation of glass transition and relaxation dynamics [154]. As shown by Mauro [155], the statistics of glass structure and bonding can be described using a (non-standard) statistical mechanical approach. This method can be used to capture both the average values of structural parameters and also fluctuations in the glass structure [156]. While research in this area is still new, eventually it

would be highly desirable to build a database of bond energies that could be used to predict the distribution of structural units in glass for complicated multi-component systems. Once theory can be used to link structure to macroscopic properties, TCT considers the glass as a network of two-body and three-body bond constraints, which may be either rigid or flexible depending on the bond energy relative to the available thermal energy in the system. At high temperatures, the network contains floppy modes that contribute to the configurational entropy of the system. As the temperature is lowered through the glass transition regime, additional bonds become rigid, thereby reducing the configurational entropy [157,158]. The number of constraints per atom (or rigidity) can be calculated analytically, and this enumeration requires a precise knowledge of the glass structure that is not always available. Therefore, constraint details (e.g. coordination numbers, the energy associated to each constraint, and mole fraction of each network-forming species) can be conveniently obtained by chemical analysis, experimental structural measurements, and through MD simulations, offering full and direct access to the structure and dynamics of the atoms within glass networks [157,158]. To this end, all these methods have been widely used to characterise the topology of borate [159–162], borosilicate [163], phosphate [164,165], borophosphate [166], and phosphosilicate glasses [167–169], i.e. many of the key families of BGs (although not specifically investigated to address bioactivity). Also, the macroscopic properties of a system, such as viscosity [170], glass transition temperature [160], or chemical durability [171,172] can then be related to the scaling of the topological constraints with composition and temperature. Mechanical properties such as hardness [173,174] and fracture toughness [175] can also be predicted using a constraint counting approach.

TCT has also been applied to model chemical reactivity, such as the dissolution kinetics of glasses. Accurately predicting the kinetics of glass dissolution is especially important for BGs because ions released from them will control most of their biological properties [26]. Pignatelli et al. [172] have used a combination of MD simulations and TCT to show that, in dilute conditions (far from saturation), the dissolution rate ( $K$ ) of silicate glasses can be predicted from the knowledge of the number of topological constraints per atom ( $n_c$ ) using the following equation [158,172]:

$$K = K_0 \exp\left[-\frac{n_c E_0}{RT}\right], \quad (1)$$

where  $K_0$  is a rate constant that depends on the solution chemistry (e.g. pH) and corresponds to the barrier-less dissolution rate of a wholly depolymerised glass (i.e. for which  $n_c = 0$ ),  $E_0 = 20\text{--}25 \text{ kJ mol}^{-1}$  an energy barrier that needs to be overcome to break a unit atomic

constraint,  $R$  the gas constant, and  $T$  the temperature. Figure 12, shows that this model is valid over a broad range of silicate-based glass compositions with a different number of constraint ( $n_c$ ) and can predict the dissolution kinetics of silicate glasses over four orders of magnitude [158].

Besides chemical reactivity, mechanical properties, such as fracture toughness, are also important characteristics of BGs. Fracture toughness represents the resistance of the glass to crack propagation under stress [12]. Bauchy et al. [175] have shown through MD simulations of sodium silicate glasses and calcium-silicate-hydrates that flexible glasses ( $n_c < 3$ ) exhibit a low overall cohesion (low surface energy) due to their low network connectivity. In contrast, stressed-rigid glasses ( $n_c > 3$ ) feature high cohesion but break in a fully brittle fashion as their high connectivity prevents any local atomic reorganisation to release stress. In turn, isostatic glasses ( $n_c = 3$ ) offer the best balance between overall cohesion and ability to release stress through local atomic reorganisations [175]. This ideal state of connectivity makes it possible for isostatic glasses to exhibit some nano-ductility (local energy dissipation), which contributes to postponing fracture. Their MD simulations showed that, in glasses, such nano-ductility manifests itself through the formation of cavities in front of the crack tip, or crack blunting [175]. This TCT-MD simulations approach could, therefore, help the computational design of tough BGs, which has long been a 'holy grail' within the bio-glass community.

In addition to the above-specialised techniques for modelling glass-forming systems, standard atomistic modelling techniques, such as MD [50] and Monte Carlo [176] can also be used. Monte Carlo techniques include Metropolis Monte Carlo, reverse Monte Carlo (RMC), and kinetic Monte Carlo (KMC) approaches. In one example, the RMC technique was used to model neutron and X-ray diffraction studies

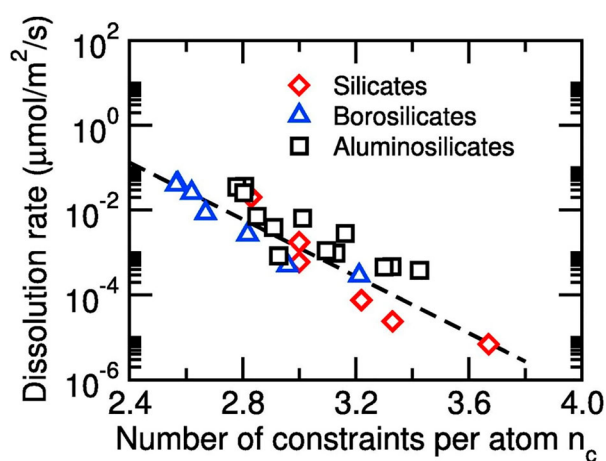


**Figure 12.** Dissolution rate of various silicate glasses as a function of the number of constraints per atom. The dashed line is the prediction from topological constraint theory (see Equation 1) [158].

of 45S5 Bioglass® [177]. The diffraction data were modelled using RMC to allow the identification of the atomic-scale structural features; the solid-state NMR data were used explicitly within the model-building process as a constraint on the connectivity of the network. The  $^{29}\text{Si}$  NMR results suggested that the host silica network mainly consists of chains and rings of  $\text{Q}^2 \text{SiO}_4$  tetrahedra, with some degree of cross-linking inferred from the presence of  $\text{Q}^3$  units. The diffraction-based RMC model revealed a Na–O distance of 2.35 Å and a corresponding coordination of  $\sim 6$ ; the coordination number was supported by the  $^{23}\text{Na}$  NMR data which suggested that the likely sodium environment is six-coordinate in the pseudo-octahedral arrangement. The RMC model provided evidence for the non-uniform distribution of Ca within the high calcium content regions of the glass [177]. These techniques can capture the structure of glassy systems and can also be used to calculate specific macroscopic properties. However, standard atomistic modelling techniques are limited in both length and time scales, making it difficult to capture the effects of thermal history on a laboratory timescale [8]. These limitations can be overcome using accelerated techniques, such as metadynamics [178], the activation-relaxation technique [179], kinetic Monte Carlo [180], energy landscape-based master equation techniques [181], or by coupling molecular dynamics results with TCT [158,182]. For example, in the pioneering works by Aertsen and co-workers [183,184] and Kerisit et al. [185,186], KMC has been shown to be a very effective simulation method to access to the long time scale required for the study of dissolution of glasses. It has been used to simulate the corrosion of glasses in aqueous solutions, a highly relevant aspect for BGs whose dissolution rate in body fluid is highly important in controlling their bioactivity or forming intimate bonding of HAp layers at the interface with the host tissues. Furthermore, Kerisit and Du have recently introduced a new approach (amorphous MC approach) in which glass structures generated from MD simulations are used as starting points for MC simulations. Correlations between dissolution rate and structural features were revealed in MC simulations of sodium borosilicate glasses covering a wide compositional range. Their findings highlighted the importance of using genuinely noncrystalline structures in MC simulations of glass dissolution rather than the classical lattice MC approach [187].

Beyond the atomic length scale, mesoscopic techniques, such as phase field modelling [188] and peridynamics [189] may also prove highly valuable for studying liquid phase separation and fracture, respectively, in glassy systems. In one study, Sanz-Herrera and Boccaccini [190] have used a larger scale numerical approach, voxel-based finite element analysis, to model the dissolution and biodegradation of a BG

scaffold for tissue engineering [190]. However, this large-scale continuum modelling, while allowing one to reach more realistic spatial and temporal scales, ignores the chemical details of the biomaterial and its bio-interfaces, such as short and medium-range structural features and elementary dynamical (ion migration and reaction) steps. All of these preliminary efforts might be extended or improved to design and enhance the characterisation of BGs, e.g. mechanical properties, which are still their ‘Achilles’ heel’!

### **Data-based modelling**

Physics-based models can, in principle, provide reliable predictions of many glass properties, and empirical modelling can supplement these theoretical approaches by making use of available experimental data. A variety of empirical models have been proposed for modelling the composition dependence of glass properties, including linear and polynomial regression [191] and ML approaches [7]. The explanatory variables in the regression models may include molar concentrations of each component of the glass or alternative representations, such as the concentrations of the presumed structural units [191]. To expand the modelling ability of complex situations, ML in general and ANNs, in particular, are promising and worth implementing. When dealing with highly complex glass compositions or biological interactions, one can indeed utilise ML. Perhaps the most potent models adopt a hybrid approach that bridges physical and empirical modelling approaches [7,191]. For example, the current trend is toward accurate MD simulations with force fields optimised through ML [192].

ANNs have been used in materials science with moderate success to predict kinetic and mechanical properties of polymers [193], the biological interaction of biopolymers [194], the glass-forming ability of metallic alloys [195,196], extract structural information from X-ray diffraction data [197], and recently the dissolution kinetics of silicate glasses [198], and glass transition temperatures,  $T_g$ , of oxide glasses [199]. The two latter properties are of great importance for the field of BGs. For example, the resulting neural network model of Cassar et al. can correctly predict, with 95% accuracy, the published  $T_g$  value with less than  $\pm 9\%$  error, whereas 90% of the data are predicted with a relative deviation lower than  $\pm 6\%$  [199]. Table 2 compares the glass transition temperature of some well-investigated BGs with the predicted values by an ANN constructed in Ref. [199].

Hence, the ANN prediction error varies from 0.5 to a maximum of 10%, whereas the experimental error can also easily reach 10% (e.g. the experimental  $T_g$  for 45S5 Bioglass® in Table 2). Furthermore, Onbaşlı et al. [209] have shown how companies like Corning Inc. used the unique advantage of developing a neural

network and genetic algorithmic models for predicting compositions that would yield the desired liquidus temperature and Young’s modulus of complex glass compositions with more than eight constituent oxides. For such development of commercial glasses, experimental measurements of the entire composition space are prohibitively expensive and time-consuming. Also, for systems with such complexity, there is no physically predictive model. There are requirements imposed on the end properties of glass and manufacturability requirements, such as appropriate liquidus temperature and a sufficiently low viscosity at a given temperature. These competing necessities are the driving force for the development of data-driven ML models of glass composition and properties [209].

Regarding fundamental glass modelling, we believe that data-driven predictive methods for chemical compositions and their corresponding physical properties offer grand opportunities to (i) develop glass compositions with improved mechanical, thermal and chemical properties, (ii) to expand or design new and exotic glass chemistries, and (iii) to find the best technological attributes [210–213]. It should be emphasised that the integration of physics-based modelling techniques (e.g. MD simulations) and data-driven approaches (e.g. ANN) can mutually inform and advance each other rather than being two independent routes. For example, high-throughput atomistic simulations offer a promising route to generate large bodies of consistent, accurate data that can be used as training sets for ML approaches. In turn, ML optimisation techniques offer a unique opportunity to develop new sets of reliable, transferable, and computationally-efficient force fields for atomistic modelling [213,214].

In the case of BGs, the interaction between glass and living tissue is currently too complicated to address from a physics-based approach. Hence, researchers still rely on empirical data. Research on BGs makes substantial use of image data, which can be interpreted using an appropriately trained neural network model to guide their optimisation. Glass article morphology (powder, fibre, monolith, scaffold, etc.) also plays an important role in governing its degree of bioactivity. Such morphology and processing effects can also be incorporated into ML-based models. Many BG compositions are too complicated to be simulated directly, but simulation techniques can inform us about the basic structural units in simplified glasses, which can be used to guide the development of new multicomponent BGs. However, data-based modelling faces many challenges. Therefore, interested readers are referred to the recent comprehensive discussion around the issues and challenges ahead of the data-driven modelling of glasses and ceramics. Still, several important issues, such as maintaining data integrity, risk of overfitting, bridging physical and empirical modelling approaches, leveraging complex data (e.g. images),

**Table 2.** Experimental glass transition temperatures ( $T_g$ ) of some well-investigated BGs [141,17] compared with values predicted by a software resulting from the ANN of Ref. [199].

Codes	Glass composition (wt.%)							Experimental $T_g$ (°C)	Predicted $T_g$ (°C) by ANN [199]	Error (%)
	Na <sub>2</sub> O	K <sub>2</sub> O	MgO	CaO	SiO <sub>2</sub>	P <sub>2</sub> O <sub>5</sub>	B <sub>2</sub> O <sub>3</sub>			
45S5	24.5	0	0	24.5	45	6	0	500 [200] 552 [204]	516	37
ICIE16	6.6	10	0	32.9	48	2.5	0	575 [200]	623	8
13-93	6	12	5	20	53	4	0	606 [201]	585	3
1-98	6	11	5	22	53	2	1	608 [202]	588	3
6P53B	10.3	2.8	10.2	18	52.7	6	0	530 [203]	578	9
S53P4	23	0	0	20	53	4	0	561 [204]	521	7
58S	0	0	0	32.6	58.2	9.2	0	785 [205]	706	10
70S30C	0	0	0	28.6	71.4	0	0	804 [206]	742	8
P50C35N15	9.3	0	0	19.7	0	71	0	420 [207]	400	5
1.5N1.5C3S + 4P	23.75	0	0	23.75	48.5	4	0	520 [208]	523	0.5

and creating interatomic potentials from ML remain to be explored [215].

## Summary and conclusions

Despite the intensive research activity, the large number of publications, and the resulting knowledge of BGs, our most critical remark is that the materials science and engineering community is only slowly embracing ML approaches, data science, and computational simulations in this field. It is likely that the complexity of the glassy state, which is defined by three nons (nonequilibrium, noncrystalline, and nonergodic), and the complex, intricate interactions of living cells with bio-glasses have been a conceptual and practical barrier to the use of modelling. However, with the continued increase of the acquired knowledge on the properties of glasses, data creation and computational power, the prospects of modelling complex problems and predicting the biological response of cells in contact with glass surfaces are achievable. We believe that modelling of BGs should be greatly stimulated and intensively applied to the design of specific aspects of glass characterisation, such as chemical degradation, mechanical properties, thermal expansion coefficient, and elastic modulus, as well as effects of porosity, morphology, etc.

ML approaches are also feasible in the context of modelling the biological response of this type of biomaterial as its ability to influence unique processes after implantation, such as protein adsorption, cell adhesion, proliferation, osteogenesis, angiogenesis, and antibacterial effects. The key challenge is to accumulate a sufficient quantity of high-quality data. The amount of data available in the field of BGs is already substantial and increasing at a rapid pace; hence, new and more efficient tools for storing, mining, cleaning, and using these data are

urgently needed. In such an effort, databases integrated with computational tools should be developed for helping the design of new BGs in a more rational and efficient manner. Currently, scattered, non-uniform experimental raw data constitutes a serious hurdle for the modelling experts. Therefore, the close engagement between experimental and theoretical groups is crucial for the field of modelling BGs to move forward. Accessible, high-quality raw experimental datasets are indispensable, as well as helping to make them more discoverable, interpretable, and reusable. As such, the full availability of experimental data and computer codes upon request is increasingly a requirement for researchers. Still, much work must be done in this regard to encourage experimentalists to share and refine valuable scientific data and push forward the 'model-based' design of BGs. To achieve this goal, cross-disciplinary collaboration among glass and data scientists, bioengineers, and clinicians in the exciting field of BGs is absolutely necessary.

## Disclosure statement

No potential conflict of interest was reported by the authors.

## Funding

The authors are grateful to the São Paulo Research Foundation [FAPESP; 2013/07793-6] – CEPID/CeRTEV – for financial support of this work and the post-doctoral fellowship granted to Maziar Montazerian [# 2015/13314-9].

## ORCID

Maziar Montazerian  <http://orcid.org/0000-0002-1409-9182>

Edgar D. Zanotto  <http://orcid.org/0000-0003-4931-4505>

John C. Mauro  <http://orcid.org/0000-0002-4319-3530>

## References

- [1] Marzari N. Materials modelling: the frontiers and the challenges. *Nat Mater.* **2016**;15(4):381–382.
- [2] Editorial. Boosting materials modelling. *Nat Mater.* **2016**;15(4):365.
- [3] Editorial. Fuelling discovery by sharing. *Nat Mater.* **2013**;12(3):173.
- [4] Zanotto ED, Mauro JC. The glassy state of matter: its definition and ultimate fate. *J Non Cryst Solids.* **2017**;471:490–495.
- [5] Zheng Q, Zhang Y, Montazerian M, et al. Understanding glass through differential scanning calorimetry. *Chem Rev.* **2019**;119(13):7848–7939.
- [6] Zanotto ED, Coutinho FAB. How many non-crystalline solids can be made from all the elements of the periodic table? *J Non Cryst Solids.* **2004**;347(1–3):285–288.
- [7] Mauro JC, Tandia A, Vargheese KD, et al. Accelerating the design of functional glasses through modeling. *Chem Mater.* **2016**;28(12):4267–4277.
- [8] Wondraczek L, Mauro JC. Advancing glasses through fundamental research. *J Eur Ceram Soc.* **2009**;29(7):1227–1234.
- [9] Mauro JC. Decoding the glass genome. *Curr Opin Solid State Mater Sci.* **2018**;22(2):58–64.
- [10] Materials innovation case study: Corning's Gorilla Glass 3 for consumer electronics. Corning Inc. Report; **2016**.
- [11] Montazerian M, Zanotto ED. A guided walk through Larry Hench's monumental discoveries. *J Mater Sci.* **2017**;52(15):8695–8732.
- [12] Hench LL. The story of Bioglass®. *J Mat Sci Mat Med.* **2006**;17(11):967–978.
- [13] Hench LL, Jones JR. Bioactive glasses: frontiers and challenges. *Front Bioeng Biotechnol.* **2015**;3:194.
- [14] Baino F, Hamzehlou S, Kargozar S. Bioactive glasses: where are we and where are we going? *J Funct Biomater.* **2018**;9(1):25.
- [15] El-Rashidy AA, Roether JA, Harhaus L, et al. Regenerating bone with bioactive glass scaffolds: a review of in vivo studies in bone defect models. *Acta Biomater.* **2017**;62:1–28.
- [16] Fu Q, Saiz E, Rahaman MN, et al. Bioactive glass scaffolds for bone tissue engineering: state of the art and future perspectives. *Mat Sci Eng C.* **2011**;31(7):1245–1256.
- [17] Rahaman MN, Day DE, Sonny Bal B, et al. Bioactive glass in tissue engineering. *Acta Biomater.* **2011**;7(6):2355–2373.
- [18] Gorustovich AA, Roether JA, Boccaccini AR. Effect of bioactive glasses on angiogenesis: a review of in vitro and in vivo evidences, tissue engineering. Part B Rev. **2010**;16(2):199–207.
- [19] Miguez-Pacheco V, Hench LL, Boccaccini AR. Bioactive glasses beyond bone and teeth: emerging applications in contact with soft tissues. *Acta Biomater.* **2015**;13:1–15.
- [20] Baino F, Novajra G, Miguez-Pacheco V, et al. Bioactive glasses: special applications outside the skeletal system. *J Non Cryst Solids.* **2016**;432:15–30.
- [21] Kargozar S, Baino F, Hamzehlou S, et al. Bioactive glasses: sprouting angiogenesis in tissue engineering. *Trends Biotechnol.* **2018**;36(4):430–444.
- [22] Kargozar S, Hamzehlou S, Baino F. Potential of bioactive glasses for cardiac and pulmonary tissue engineering. *Materials.* **2017**;10(12):1429.
- [23] Gorustovich AA, Roether JA, Boccaccini AR. Effect of bioactive glasses on angiogenesis: a review of in vitro and in vivo evidences, tissue engineering. Part B Rev. **2010**;16(2):199–207.
- [24] Fernandes JS, Gentile P, Pires RA, et al. Multifunctional bioactive glass and glass-ceramic biomaterials with antibacterial properties for repair and regeneration of bone tissue. *Acta Biomater.* **2017**;59:2–11.
- [25] Polak J, Hench L. Gene therapy progress and prospects: in tissue engineering. *Gene Ther.* **2005**;12(24):1725–1733.
- [26] Hoppe A, Güldal NS, Boccaccini AR. A review of the biological response to ionic dissolution products from bioactive glasses and glass-ceramics. *Biomaterials.* **2011**;32(11):2757–2774.
- [27] Rabiee SM, Nazparvar N, Azizian M, et al. Effect of ion substitution on properties of bioactive glasses: a review. *Ceram Int.* **2015**;41(6):7241–7251.
- [28] Hoppe A, Boccaccini AR. Chapter 16: bioactive glasses as carriers of therapeutic ions and the biological implications. *RSC Smart Mater.* **2017**;23:362–392.
- [29] Wu C, Chang J. Mesoporous bioactive glasses: structure characteristics, drug/growth factor delivery and bone regeneration application. *Interface Focus.* **2012**;2(3):292–306.
- [30] Baino F, Fiorilli S, Vitale-Brovarone C. Bioactive glass-based materials with hierarchical porosity for medical applications: review of recent advances. *Acta Biomater.* **2016**;42:18–32.
- [31] Kargozar S, Montazerian M, Hamzehlou S, et al. Mesoporous bioactive glasses: promising platforms for antibacterial strategies. *Acta Biomater.* **2018**;81:1–19.
- [32] Zhou Y, Shi M, Jones JR, et al. Strategies to direct vascularisation using mesoporous bioactive glass-based biomaterials for bone regeneration. *Int Mat Rev.* **2017**;62(7):392–414.
- [33] Montazerian M, Zanotto ED. Bioactive and inert dental glass-ceramics. *J Bio Mat Res – Part A.* **2017**;105(2):619–639.
- [34] Montazerian M, Zanotto ED. History and trends of bioactive glass-ceramics. *J Bio Mat Res – Part A.* **2016**;104(5):1231–1249.
- [35] Sola A, Bellucci D, Cannillo V, et al. Bioactive glass coatings: a review. *Surf Eng.* **2011**;27(8):560–572.
- [36] Bellucci D, Sola A, Cannillo V. Hydroxyapatite and tricalcium phosphate composites with bioactive glass as second phase: state of the art and current applications. *J Biomed Mater Res – Part A.* **2016**;104(4):1030–1056.
- [37] Jones JR. Review of bioactive glass: from Hench to hybrids. *Acta Biomater.* **2013**;9(1):4457–4486.
- [38] Miola M, Pakzad Y, Banijamali S, et al. Glass-ceramics for cancer treatment: so close, or yet so far? *Acta Biomater.* **2018**;83:55–70.
- [39] Day DE. Glasses for radiotherapy. In: Jones JR, Clare AG, editors. *Bio-glasses: an introduction*. Chichester, United Kingdom: John Wiley & Sons, Inc.; **2012**. p. 203–228.
- [40] Hench LL. Opening paper 2015- some comments on bioglass: four eras of discovery and development. *Biomedical Glasses.* **2015**;1(1):1–11.
- [41] Kargozar S, Baino F, Hamzehlou S, et al. Bioactive glasses entering the mainstream. *Drug Discov Today.* **2018**;23(10):1700–1704.

- [42] Kargozar S, Montazerian M, Fiume E, et al. Multiple and promising applications of Sr-containing bioactive glasses in bone tissue engineering. *Front Bioeng Biotechnol Biomater.* **2019**;7:161.
- [43] Allen MP, Tildesley DJ. *Computer simulation of liquids*. 2nd ed. New York, United States: Oxford University Press; **2017**.
- [44] Dresselhaus MS, Lee YP, Ossi PM, et al. Molecular dynamics simulation of silicate glasses. *Top Appl Phys.* **2017**;132:415–458.
- [45] Du J, Rimsza J. Atomistic computer simulations of water interactions and dissolution of inorganic glasses. *Mater Degrad.* **2017**;1:16.
- [46] Hahn SH, Rimsza J, Criscenti L, et al. Development of a ReaxFF reactive force field for NaSiO<sub>x</sub>/water systems and its application to sodium and proton self-diffusion. *J Phys Chem C.* **2018**;122(34):19613–19624.
- [47] Deng L, Miyatani K, Amma S-I, et al. Reaction mechanisms and interfacial behaviors of sodium silicate glass in an aqueous environment from reactive force field-based molecular dynamics simulations. *J Phys Chem C.* **2019**;123(35):21538–21547.
- [48] Massobrio C, Du J, Bernasconi M, et al., editors. *Molecular dynamics simulations of disordered materials*. Cham, Switzerland: Springer Nature; **2015**.
- [49] Tilocca A. Structural models of bioactive glasses from molecular dynamics simulations. *Proc Royal Soc.* **2009**;465:1003–1027.
- [50] Tilocca A. Chapter 4: molecular dynamics simulations of bioactive glass structure and in vitro reactivity. *RSC Smart Mater.* **2017**;23:89–104.
- [51] Tilocca A. Current challenges in atomistic simulations of glasses for biomedical applications. *Phys Chem Chem Phys.* **2014**;16(9):3874–3880.
- [52] Senftle TP, Hong S, Islam MM, et al. The ReaxFF reactive force-field: development, applications and future directions. *NPJ Comp Mat.* **2016**;2:15011.
- [53] Rimsza JM, Yeon J, Van Duin ACT, et al. Water interactions with nanoporous silica: comparison of ReaxFF and ab initio based molecular dynamics simulations. *J Phys Chem C.* **2016**;120(43):24803–24816.
- [54] Yu Y, Wang B, Wang M, et al. Revisiting silica with ReaxFF: towards improved predictions of glass structure and properties via reactive molecular dynamics. *J Non Cryst Solids.* **2016**;443:148–154.
- [55] Chowdhury SC, Haque BZG, Gillespie JW. Molecular dynamics simulations of the structure and mechanical properties of silica glass using ReaxFF. *J Mater Sci.* **2016**;51(22):10139–10159.
- [56] Yu Y, Wang B, Wang M, et al. Reactive molecular dynamics simulations of sodium silicate glasses – toward an improved understanding of the structure. *Int J Appl Glass Sci.* **2017**;8(3):276–284.
- [57] Christie JK, Ainsworth RI, Hernandez SER, et al. Structures and properties of phosphate-based bioactive glasses from computer simulation: a review. *J Mat Chem B.* **2017**;5(27):5297–5306.
- [58] Pedone A, Menziani MC. What can we learn from atomistic simulations of bioactive glasses? *Adv Str Mat.* **2016**;53:119–145.
- [59] Tilocca A, De Leeuw NH. Ab initio molecular dynamics study of 45S5 bioactive silicate glass. *J Phys Chem B.* **2006**;110(51):25810–25816.
- [60] Tilocca A. Structure and dynamics of bioactive phosphosilicate glasses and melts from ab initio molecular dynamics simulations. *Phys Rev B – Condens Matter Mater Phys.* **2007**;76(22):224202.
- [61] Tilocca A. Short- and medium-range structure of multicomponent bioactive glasses and melts: an assessment of the performances of shell-model and rigid-ion potentials. *J Chem Phys.* **2008**;129(8):084504.
- [62] Tilocca A. Cooling rate and size effects on the medium-range structure of multicomponent oxide glasses simulated by molecular dynamics. *J Chem Phys.* **2013**;139(11):114501.
- [63] Vollmayr K, Kob W, Binder K. Cooling-rate effects in amorphous silica: a computer-simulation study. *Phys Rev B Condensed Matter Mater Phys.* **1996**;54(22):15808–15827.
- [64] Pedone A, Charpentier T, Malavasi G, et al. New insights into the atomic structure of 45S5 Bioglass by means of solid-state NMR spectroscopy and accurate first-principles simulations. *Chem Mat.* **2010**;22(19):5644–5652.
- [65] Stevansson B, Mathew R, Edén M. Assessing the phosphate distribution in bioactive phosphosilicate glasses by <sup>31</sup>P solid-state NMR and molecular dynamics simulations. *J Phys Chem B.* **2014**;118(29):8863–8876.
- [66] Linati L, Lusvardi G, Malavasi G, et al. Medium-range order in phospho-silicate bioactive glasses: insights from MAS-NMR spectra, chemical durability experiments and molecular dynamics simulations. *J Non Cryst Solids.* **2008**;354(2–9):84–89.
- [67] Bhaskar P, Maurya Y, Kumar R, et al. Cooling rate effects on the structure of 45S5 Bioglass: computational and experimental evidence of Si–P avoidance. *Cond Mat Mtrl Sci.* arXiv:1906.10111v1.
- [68] Lu X, Deng L, Huntley C, et al. Mixed network former effect on structure, physical properties, and bioactivity of 45S5 bioactive glasses: an integrated experimental and molecular dynamics simulation study. *J Phys Chem B.* **2018**;122(9):2564–2577.
- [69] Mead RN, Mountjoy G. Modeling the local atomic structure of bioactive sol-gel-derived calcium silicates. *Chem Mat.* **2006**;18(17):3956–3964.
- [70] Malavasi G, Menabue L, Menziani MC, et al. New insights into the bioactivity of SiO<sub>2</sub>–CaO and SiO<sub>2</sub>–CaO–P<sub>2</sub>O<sub>5</sub> sol-gel glasses by molecular dynamics simulations. *J Solgel Sci Technol.* **2013**;67(1):208–219.
- [71] Côté AS, Cormack AN, Tilocca A. Influence of calcium on the initial stages of the sol-gel synthesis of bioactive glasses. *J Phys Chem B.* **2016**;120(45):11773–11780.
- [72] Mathew R, Stevansson B, Tilocca A, et al. Toward a rational design of bioactive glasses with optimal structural features: composition-structure correlations unveiled by solid-state NMR and MD simulations. *J Phys Chem B.* **2014**;118(3):833–844.
- [73] Mathew R, Stevansson B, Edén M. Na/Ca Intermixing around silicate and phosphate groups in bioactive phosphosilicate glasses revealed by Heteronuclear solid-state NMR and molecular dynamics simulations. *J Phys Chem B.* **2015**;119(17):5701–5715.
- [74] Berardo E, Corno M, Cormack AN, et al. Probing the fate of interstitial water in bulk bioactive glass by ab initio simulations. *RSC Adv.* **2014**;4(69):36425–36436.
- [75] Pedone A, Tavanti F, Malavasi G, et al. An atomic-level look at the structure-property relationship of

- cerium-doped glasses using classical molecular dynamics. *J Non Cryst Solids*. 2018;498:331–337.
- [76] Benedetti F, Luches P, D'Addato S, et al. Structure of active cerium sites within bioactive glasses. *J American Ceram Soc*. 2017;100(11):5086–5095.
- [77] Pedone A, Malavasi G, Menziani MC. Computational insight into the effect of CaO/MgO substitution on the structural properties of phospho-silicate bioactive glasses. *J Phys Chem C*. 2009;113(35):15723–15730.
- [78] Pedone A, Chen X, Hill RG, et al. Molecular dynamics investigation of Halide-containing Phospho-silicate bioactive glasses. *J Phys Chem B*. 2018;122(11):2940–2948.
- [79] Christie JK, Brauer DS. The role of fluoride in the nanoheterogeneity of bioactive glasses. *Phys Chem Glasses Euro J Glass Sci Technol Part B*. 2017;58(4):180–186.
- [80] Shaharyar Y, Wein E, Kim J-J, et al. Structure-solubility relationships in fluoride-containing phosphate based bioactive glasses. *J Mat Chem B*. 2015;3(48):9360–9373.
- [81] Christie JK, Ainsworth RI, de Leeuw NH. Ab initio molecular dynamics simulations of structural changes associated with the incorporation of fluorine in bioactive phosphate glasses. *Biomaterials*. 2014;35(24):6164–6171.
- [82] Pedone A, Charpentier T, Menziani MC. The structure of fluoride-containing bioactive glasses: new insights from first-principles calculations and solid state NMR spectroscopy. *J Mater Chem*. 2012;22(25):12599–12608.
- [83] Christie JK, Pedone A, Menziani MC, et al. Fluorine environment in bioactive glasses: ab initio molecular dynamics simulations. *J Phys Chem B*. 2011;115(9):2038–2045.
- [84] Lusvardi G, Malavasi G, Tarsitano F, et al. Quantitative structure-property relationships of potentially bioactive fluoro phospho-silicate glasses. *J Phys Chem B*. 2009;113(30):10331–10338.
- [85] Lusvardi G, Malavasi G, Cortada M, et al. Elucidation of the structural role of fluorine in potentially bioactive glasses by experimental and computational investigation. *J Phys Chem B*. 2008;112(40):12730–12739.
- [86] Xiang Y, Du J, Skinner LB, et al. Structure and diffusion of ZnO-SrO-CaO-Na<sub>2</sub>O-SiO<sub>2</sub> bioactive glasses: a combined high energy X-ray diffraction and molecular dynamics simulations study. *RSC Adv*. 2013;3(17):5966–5978.
- [87] Lusvardi G, Malavasi G, Menabue L, et al. Properties of zinc releasing surfaces for clinical applications. *J Biomater Appl*. 2008;22(6):505–526.
- [88] Malavasi G, Lusvardi G, Pedone A, et al. Crystallization kinetics of bioactive glasses in the ZnO-Na<sub>2</sub>O-CaO-SiO<sub>2</sub> system. *J Phys Chem A*. 2007;111(34):8401–8408.
- [89] Ren M, Lu X, Deng L, et al. B<sub>2</sub>O<sub>3</sub>/SiO<sub>2</sub> substitution effect on structure and properties of Na<sub>2</sub>O-CaO-SrO-P<sub>2</sub>O<sub>5</sub>-SiO<sub>2</sub> bioactive glasses from molecular dynamics simulations. *Phys Chem Chem Phys*. 2018;20(20):14090–14104.
- [90] Stevansson B, Yu Y, Edén M. Structure-composition trends in multicomponent borosilicate-based glasses deduced from molecular dynamics simulations with improved B-O and P-O force fields. *Phys Chem Chem Phys*. 2018;20(12):8192–8209.
- [91] Lu X, Deng L, Kuo P-H, et al. Effects of boron oxide substitution on the structure and bioactivity of SrO-containing bioactive glasses. *J Mater Sci*. 2017;52(15):8793–8811.
- [92] Yu Y, Stevansson B, Edén M. Medium-range structural organization of phosphorus-bearing borosilicate glasses revealed by advanced solid-state NMR experiments and MD simulations: consequences of B/Si substitutions. *J Phys Chem B*. 2017;121(41):9737–9752.
- [93] Du J, Xiang Y. Investigating the structure-diffusion-bioactivity relationship of strontium containing bioactive glasses using molecular dynamics based computer simulations. *J Non Cryst Solids*. 2016;432:35–40.
- [94] Du J, Xiang Y. Effect of strontium substitution on the structure, ionic diffusion and dynamic properties of 45S5 bioactive glasses. *J Non Cryst Solids*. 2012;358(8):1059–1071.
- [95] Xiang Y, Du J. Effect of strontium substitution on the structure of 45S5 Bioglasses. *Chem Mat*. 2011;23(11):2703–2717.
- [96] Malavasi G, Pedone A, Menziani MC. Study of the structural role of gallium and aluminum in 45S5 bioactive glasses by molecular dynamics simulations. *J Phys Chem B*. 2013;117(15):4142–4150.
- [97] Christie JK, Ainsworth RI, De Leeuw NH. Investigating structural features which control the dissolution of bioactive phosphate glasses: beyond the network connectivity. *J Non Cryst Solids*. 2016;432:31–34.
- [98] Broglia G, Mugoni C, Siligardi C, et al. Lithium and copper transport properties in phosphate glasses: a molecular dynamics study. *J Non Cryst Solids*. 2018;481:522–529.
- [99] Gross TM, Lahiri J, Golas A, et al. Copper-containing glass ceramic with high antimicrobial efficacy. *Nat Commun*. 2019;10(1):1979.
- [100] Voigt U, Lammert H, Eckert H, et al. Cation clustering in lithium silicate glasses: quantitative description by solid-state NMR and molecular dynamics simulations. *Phys Rev B – Condens Matter Mater Phys*. 2005;72(6):064207.
- [101] Christie JK, Cormack AN, Hanna JV, et al. Bioactive sol-gel glasses at the atomic scale: the complementary use of advanced probe and computer modeling methods. *Int J Appl Glass Sci*. 2016;7(2):147–153.
- [102] Côté AS, Cormack AN, Tilocca A. Reactive molecular dynamics: an effective tool for modelling the sol-gel synthesis of bioglasses. *J Mater Sci*. 2017;52(15):9006–9013.
- [103] Eckert H. Structural characterization of bioactive glasses by solid state NMR. *J Solgel Sci Technol*. 2018;88(2):263–295.
- [104] Tilocca A, Cormack AN. The initial stages of Bioglass dissolution: a Car-Parrinello molecular-dynamics study of the glass-water interface. *Proc Royal Soc A Math Phys Eng Sci*. 2011;467(2131):2102–2111.
- [105] Tilocca A. Atomic-scale models of early-stage alkali depletion and SiO<sub>2</sub>-rich gel formation in bioactive glasses. *Phys Chem Chem Phys*. 2015;17(4):2696–2702.
- [106] Zeitler TR, Cormack AN. Interaction of water with bioactive glass surfaces. *J Cryst Growth*. 2006;294(1):96–102.
- [107] Tilocca A, Cormack AN, De Leeuw NH. The structure of bioactive silicate glasses: new insight from

- molecular dynamics simulations. *Chem Mat.* **2007**;19(1):95–103.
- [108] Tilocca A, Cormack AN. Structural effects of phosphorus inclusion in bioactive silicate glasses. *J Phys Chem B.* **2007**;111(51):14256–14264.
- [109] Tilocca A, Cormack AN. Exploring the surface of bioactive glasses: water adsorption and reactivity. *J Phys Chem C.* **2008**;112(31):11936–11945.
- [110] Tilocca A, Cormack AN. Modeling the water-bio-glass interface by ab initio molecular dynamics simulations. *ACS Appl Mat Int.* **2009**;1(6):1324–1333.
- [111] Tilocca A, Cormack AN. Surface signatures of bioactivity: MD simulations of 45S and 65S silicate glasses. *Langmuir.* **2010**;26(1):545–551.
- [112] Leed EA, Sofo JO, Pantano CG. Electronic structure calculations of physisorption and chemisorption on oxide glass surfaces. *Phys Rev B – Condens Matter Mater Phys.* **2005**;72(15):155427.
- [113] Christie JK, Ainsworth RI, Di Tommaso D, et al. Nanoscale chains control the solubility of phosphate glasses for biomedical applications. *J Phys Chem B.* **2013**;117(36):10652–10657.
- [114] Tilocca A. Realistic models of bioactive glass radioisotope vectors in practical conditions: structural effects of ion exchange. *J Phys Chem C.* **2015**;119(49):27442–27448.
- [115] Christie JK, Tilocca A. Integrating biological activity into radioisotope vectors: molecular dynamics models of yttrium-doped bioactive glasses. *J Mater Chem.* **2012**;22(24):12023–12031.
- [116] Christie JK, Malik J, Tilocca A. Bioactive glasses as potential radioisotope vectors for in situ cancer therapy: investigating the structural effects of yttrium. *Phys Chem Chem Phys.* **2011**;13(39):17749–17755.
- [117] Lin Y, Mauro JC, Kaur G. Bioactive glasses for cancer therapy. In: Kaur G, editor. *Biomedical, therapeutic and clinical applications of bioactive glasses.* Amsterdam, Netherlands: Elsevier; **2019.** p. 273–312. Woodhead Publishing Series in Biomaterials.
- [118] Tilocca A. Sodium migration pathways in multicomponent silicate glasses: Car-Parrinello molecular dynamics simulations. *J Chem Phys.* **2010**;133(1):014701.
- [119] Smith W, Forester TR, Greaves GN, et al. Molecular dynamics simulation of alkali-metal diffusion in alkali-metal disilicate glasses. *J Mater Chem.* **1997**;7(2):331–336.
- [120] Pedone A, Malavasi G, Cristina Menziani M, et al. Role of magnesium in soda-lime glasses: insight into structural, transport, and mechanical properties through computer simulations. *J Phys Chem C.* **2008**;112(29):11034–11041.
- [121] Car R, Parrinello M. Unified approach for molecular dynamics and density-functional theory. *Phys Rev Lett.* **1985**;55(22):2471–2474.
- [122] Cormack AN, Du J, Zeidler TR. Alkali ion migration mechanisms in silicate glasses probed by molecular dynamics simulations. *Phys Chem Chem Phys.* **2002**;4(14):3193–3197.
- [123] Tilocca A. Dynamical descriptors of bioactivity: a correlation between chemical durability and ion migration in biodegradable glasses. *Phys Chem Chem Phys.* **2017**;19(9):6334–6337.
- [124] Obata A, Nakamura S, Yamashita K. Interpretation of electrical polarization and depolarization mechanisms of bioactive glasses in relation to ionic migration. *Biomater.* **2004**;25(21):5163–5169.
- [125] Tilocca A. Molecular dynamics simulations of a bioactive glass nanoparticle. *J Mater Chem.* **2011**;21(34):12660–12667.
- [126] Brunner TJ, Grass RN, Stark WJ. Glass and bioglass nanopowders by flame synthesis. *Chem Comm.* **2006**;13:1384–1386.
- [127] Pedone A, Muniz-Miranda F, Tilocca A, et al. The antioxidant properties of Ce-containing bioactive glass nanoparticles explained by molecular dynamics simulations. *Biomed Glas.* **2016**;2(1):19–28.
- [128] Nicolini V, Varini E, Malavasi G, et al. The effect of composition on structural, thermal, redox and bioactive properties of Ce-containing glasses. *Mat Des.* **2016**;97:73–85.
- [129] Nicolini V, Gambuzzi E, Malavasi G, et al. Evidence of catalase mimetic activity in Ce<sup>3+</sup>/Ce<sup>4+</sup> doped bioactive glasses. *J Phys Chem B.* **2015**;119(10):4009–4019.
- [130] Butler KT, Davies DW, Cartwright H, et al. Machine learning for molecular and materials science. *Nature.* **2018**;559(7715):547–555.
- [131] Le TC, Winkler DA. Discovery and optimization of materials using evolutionary approaches. *Chem Rev.* **2016**;116(10):6107–6132.
- [132] Liu Y, Zhao T, Ju W, et al. Materials discovery and design using machine learning. *J Materiomics.* **2017**;3(3):159–177.
- [133] Ramprasad R, Batra R, Paliani G, et al. Machine learning in materials informatics: recent applications and prospects. *NPJ Comput Mat.* **2017**;3(1):54.
- [134] Kohn J. New approaches to biomaterials design. *Nat Mater.* **2004**;3(11):745–747.
- [135] Kohn J, Welsh WJ, Knight D. A new approach to the rationale discovery of polymeric biomaterials. *Biomater.* **2007**;28(29):4171–4177.
- [136] Brauer DS, Rüssel C, Kraft J. Solubility of glasses in the system P<sub>2</sub>O<sub>5</sub>-CaO-MgO-Na<sub>2</sub>O-TiO<sub>2</sub>: experimental and modeling using artificial neural networks. *J Non Cryst Solids.* **2007**;353(3):263–270.
- [137] Echezarreta-López MM, Landin M. Using machine learning for improving knowledge on antibacterial effect of bioactive glass. *Int J Pharm.* **2013**;453(2):641–647.
- [138] Yilmaz C, Ustun D, Akdagli A. Usage of artificial neural network for estimating of the electrospun nanofiber diameter. *IDAP 2017 - International Artificial Intelligence and Data Processing Symposium.* 2017. DOI:10.1109/IDAP.2017.8090329.
- [139] Sha W, Edwards KL. The use of artificial neural networks in materials science based research. *Mat Des.* **2007**;28(6):1747–1752.
- [140] Farano V, Maurin J-C, Attik N, et al. Sol-gel bio-glasses in dental and periodontal regeneration: a systematic review. *J Biomed Mat Res – Part B.* **2018**;107B:1210–1227.
- [141] Fu Q, Mauro JC, Rahaman MN. Bioactive glass innovations through academia-industry collaboration. *Int J Appl Glass Sci.* **2016**;7(2):139–146.
- [142] Košťál P, Šhánělová J, Málek J. Viscosity of chalcogenide glass-formers. *Int Mat Rev.* **2019.** DOI:10.1080/09506608.2018.1564545.
- [143] Lumeau J, Zanotto ED. A review of the photo-thermal mechanism and crystallization of photo-thermorefractive (PTR) glass. *Int Mat Rev.* **2017**;62(6):348–366.



- [144] Shi Y. Size-dependent mechanical responses of metallic glasses. *Int Mat Rev.* **2019**;64(3):163–180.
- [145] Zanotto ED, Tsuchida JE, Schneider JF, et al. Thirty-year quest for structure-nucleation relationships in oxide glasses. *Int Mat Rev.* **2015**;60(7):376–391.
- [146] Mauro JC, Allan DC, Potuzak M. Nonequilibrium viscosity of glass. *Phys Rev B – Condens Matter Mater Phys.* **2009**;80(9):094204.
- [147] Mauro JC, Loucks RJ, Gupta PK. Fictive temperature and the glassy state. *J Am Ceram Soc.* **2009**;92(1):75–86.
- [148] Gupta PK, Mauro JC. The laboratory glass transition. *J Chem Phys.* **2007**;126(22):224504.
- [149] Mauro JC, Smedskjaer MM. Statistical mechanics of glass. *J Non Cryst Solids.* **2014**;396–397:41–53.
- [150] Mauro JC, Gupta PK, Loucks RJ. Continuously broken ergodicity. *J Chem Phys.* **2007**;126(18):184511.
- [151] Debenedetti PG, Stillinger FH. Supercooled liquids and the glass transition. *Nature.* **2001**;410(6825):259–267.
- [152] Mauro JC, Loucks RJ, Varshneya AK, et al. Enthalpy landscapes and the glass transition. *Sci Model Simul SMNS.* **2008**;15(1–3):241–281.
- [153] Odagaki T. Non-equilibrium statistical mechanics based on the free energy landscape and its application to glassy systems. *J Phys Soc Japan.* **2017**;86(8):082001.
- [154] Mauro JC, Loucks RJ. Selenium glass transition: a model based on the enthalpy landscape approach and nonequilibrium statistical mechanics. *Phys Rev B – Condens Matter Mater Phys.* **2007**;76(17):174202.
- [155] Mauro JC. Statistics of modifier distributions in mixed network glasses. *J Chem Phys.* **2013**;138(12):12A522.
- [156] Kirchner KA, Kim SH, Mauro JC. Statistical mechanics of topological fluctuations in glass-forming liquids. *Phys A Stat Mech Appl.* **2018**;510:787–801.
- [157] Mauro JC. Topological constraint theory of glass. *Am Ceram Soc Bull.* **2011**;90(4):31–37.
- [158] Bauchy M. Deciphering the atomic genome of glasses by topological constraint theory and molecular dynamics: a review. *Comp Mat Sci.* **2019**;159:95–102.
- [159] Gupta PK, Mauro JC. Composition dependence of glass transition temperature and fragility. I. A topological model incorporating temperature-dependent constraints. *J Chem Phys.* **2009**;130(9):094503.
- [160] Mauro JC, Gupta PK, Loucks RJ. Composition dependence of glass transition temperature and fragility. II. A topological model of alkali borate liquids. *J Chem Phys.* **2009**;130(23):234503.
- [161] Smedskjaer MM, Mauro JC, Sen S, et al. Impact of network topology on cationic diffusion and hardness of borate glass surfaces. *J Chem Phys.* **2010**;133(15):154509.
- [162] Smedskjaer MM, Mauro JC, Sen S, et al. Quantitative design of glassy materials using temperature-dependent constraint theory. *Chem Mat.* **2010**;22(18):5358–5365.
- [163] Smedskjaer MM, Mauro JC, Youngman RE, et al. Topological principles of borosilicate glass chemistry. *J Phys Chem B.* **2011**;115(44):12930–12946.
- [164] Fu AI, Mauro JC. Topology of alkali phosphate glass networks. *J Non Cryst Solids.* **2013**;361(1):57–62.
- [165] Hermansen C, Mauro JC, Yue Y. A model for phosphate glass topology considering the modifying ion sub-network. *J Chem Phys.* **2014**;140(15):154501.
- [166] Hermansen C, Youngman RE, Wang J, et al. Structural and topological aspects of borophosphate glasses and their relation to physical properties. *J Chem Phys.* **2015**;142(18):184503.
- [167] Zeng H, Jiang Q, Liu Z, et al. Unique sodium phosphosilicate glasses designed through extended topological constraint theory. *J Phys Chem B.* **2014**;118(19):5177–5183.
- [168] Jiang Q, Zeng H, Li X, et al. Tailoring sodium silicophosphate glasses containing SiO<sub>6</sub>-octahedra through structural rules and topological principles. *J Chem Phys.* **2014**;141(12):4896150.
- [169] Hermansen C, Guo X, Youngman RE, et al. Structure-topology-property correlations of sodium phosphosilicate glasses. *J Chem Phys.* **2015**;143(6):064510.
- [170] Mauro JC, Ellison AJ, Allan DC, et al. Topological model for the viscosity of multicomponent glass-forming liquids. *Int J Appl Glass Sci.* **2013**;4(4):408–413.
- [171] Mascaraque N, Bauchy M, Smedskjaer MM. Correlating the network topology of oxide glasses with their chemical durability. *J Phys Chem B.* **2017**;121(5):1139–1147.
- [172] Pignatelli I, Kumar A, Bauchy M, et al. Topological control on silicates' dissolution kinetics. *Langmuir.* **2016**;32(18):4434–4439.
- [173] Smedskjaer MM, Mauro JC, Yue Y. Prediction of glass hardness using temperature-dependent constraint theory. *Phys Rev Lett.* **2010**;105(11):115503.
- [174] Zheng Q, Yue Y, Mauro JC. Density of topological constraints as a metric for predicting glass hardness. *Appl Phys Lett.* **2017**;111:011907.
- [175] Bauchy M, Wang B, Wang M, et al. Fracture toughness anomalies: viewpoint of topological constraint theory. *Acta Mater.* **2016**;121:234–239.
- [176] Mauro JC, Varshneya AK. Multiscale modeling of arsenic selenide glass. *J Non Cryst Solids.* **2007**;353(13–15):1226–1231.
- [177] FitzGerald V, Pickup DM, Greenspan D, et al. A neutron and X-ray diffraction study of Bioglass® with reverse Monte Carlo modelling. *Adv Funct Mater.* **2007**;17(18):3746–3753.
- [178] Kushima A, Eapen J, Li J, et al. Time scale bridging in atomistic simulation of slow dynamics: viscous relaxation and defect activation. *European Phys J B.* **2011**;82(3–4):271–293.
- [179] Mousseau N, Barkema GT. Traveling through potential energy landscapes of disordered materials: The activation-relaxation technique. *Phys Rev – Stat Phys Plasmas Fluids Relat Interdiscip Top.* **1998**;57(2):2419–2424.
- [180] Mauro JC, Du J. Achieving long time scale simulations of glass-forming systems. *Comp Theor Chem.* **2012**;987:122–133.
- [181] Mauro JC, Loucks RJ, Gupta PK. Metabasin approach for computing the master equation dynamics of systems with broken ergodicity. *J Phys Chem A.* **2007**;111(32):7957–7965.
- [182] Bauchy M, Micoulaut M. Atomic scale foundation of temperature-dependent bonding constraints in network glasses and liquids. *J Non Cryst Solids.* **2011**;357(14):2530–2537.
- [183] Aertsens M, Van Iseghem P. Modelling glass dissolution with a Monte Carlo technique. *Mat Res Soc Symp – Proc.* **1996**;412:271–278.
- [184] Aertsens M. Testing the Grambow glass dissolution model by comparing it with Monte Carlo

- simulation results. *Mat Res Soc Symp – Proc.* **1999**; 556:409–419.
- [185] Kerisit S, Ryan JV, Pierce EM. Monte Carlo simulations of the corrosion of aluminoborosilicate glasses. *J Non Cryst Solids.* **2013**;378:273–281.
- [186] Kerisit S, Pierce EM, Ryan JV. Monte Carlo simulations of coupled diffusion and surface reactions during the aqueous corrosion of borosilicate glasses. *J Non Cryst Solids.* **2015**;408:142–149.
- [187] Kerisit S, Du J. Monte Carlo simulation of borosilicate glass dissolution using molecular dynamics-generated glass structures. *J Non Cryst Solids.* **2019**;522:119601.
- [188] Chen L-Q. Phase-field models for microstructure evolution. *Annual Rev Mat Sci.* **2002**;32:113–140.
- [189] Ha YD, Bobaru F. Characteristics of dynamic brittle fracture captured with peridynamics. *Eng Fract Mech.* **2011**;78(6):1156–1168.
- [190] Sanz-Herrera JA, Boccaccini AR. Modelling bioactivity and degradation of bioactive glass based tissue engineering scaffolds. *Int J Solids Struct.* **2011**;48(2):257–268.
- [191] Priven AI. General method for calculating the properties of oxide glasses and glass forming melts from their composition and temperature. *Glass Technol.* **2004**;45(6):244–254.
- [192] Chmiela S, Sauceda HE, Müller K-R, et al. Towards exact molecular dynamics simulations with machine-learned force fields. *Nat Commun.* **2018**;9(1):3887.
- [193] Zhang Z, Friedrich K. Artificial neural networks applied to polymer composites: a review. *Compos Sci Technol.* **2003**;63(14):2029–2044.
- [194] Ebube NK, Owusu-Ababio G, Adeyeye CM. Preformulation studies and characterization of the physicochemical properties of amorphous polymers using artificial neural networks. *Int J Pharm.* **2000**;196(1):27–35.
- [195] Ren F, Ward L, Williams T, et al. Accelerated discovery of metallic glasses through iteration of machine learning and high-throughput experiments. *Sci Adv.* **2018**;4(4):eaq1566.
- [196] Cai A-H, Xiong X, Liu Y, et al. Artificial neural network modeling for undercooled liquid region of glass forming alloys. *Comp Mat Sci.* **2010**;48(1):109–114.
- [197] Ziletti A, Kumar D, Scheffler M, et al. The face of crystals: insightful classification using deep learning. *Cond-Mat.* ArXiv:1709.02298. **2017**. <http://arxiv.org/abs/1709.02298>.
- [198] Anoop Krishnan NM, Mangalathu S, Smedskjaer MM, et al. Predicting the dissolution kinetics of silicate glasses using machine learning. *J Non Cryst Solids.* **2018**;487:37–45.
- [199] Cassar DR, Carvalho ACPLF, Zanotto ED. Predicting glass transition temperatures using neural networks. *Acta Mater.* **2018**;159:249–256.
- [200] Wu ZY, Hill RG, Yue S, et al. Melt-derived bioactive glass scaffolds produced by a gel-cast foaming technique. *Acta Biomater.* **2011**;7(4):1807–1816.
- [201] Fu Q, Rahaman MN, Bal BS, et al. Preparation and bioactive characteristics of a porous 13-93 glass, and fabrication into the articulating surface of a proximal tibia. *J Biomed Mat Res – Part A.* **2007**;82(1):222–229.
- [202] Fagerlund S, Massera J, Hupa M, et al. T-T-T behaviour of bioactive glasses 1-98 and 13-93. *J European Ceram Soc.* **2012**;32(11):2731–2738.
- [203] Fu Q, Saiz E, Tomsia AP. Bioinspired strong and highly porous glass scaffolds. *Adv Funct Mat.* **2011**;21(6):1058–1063.
- [204] Massera J, Fagerlund S, Hupa L, et al. Crystallization mechanism of the bioactive glasses, 45S5 and S53P4. *J Am Ceram Soc.* **2012**;95(2):607–613.
- [205] Arcos D, Greenspan DC, Vallet-Regí M. Influence of the stabilization temperature on textural and structural features and ion release in SiO<sub>2</sub>-CaO-P<sub>2</sub>O<sub>5</sub> sol-gel glasses. *Chem Mat.* **2002**;14(4):1515–1522.
- [206] Jones JR, Ehrenfried LM, Hench LL. Optimising bioactive glass scaffolds for bone tissue engineering. *Biomater.* **2006**;27(7):964–973.
- [207] Ahmed I, Lewis M, Olsen I, et al. Phosphate glasses for tissue engineering: part 1. Processing and characterisation of a ternary-based P<sub>2</sub>O<sub>5</sub>-CaO-Na<sub>2</sub>O glass system. *Biomater.* **2004**;25(3):491–499.
- [208] Peitl O, Zanotto ED, Serbena FC, et al. Compositional and microstructural design of highly bioactive P<sub>2</sub>O<sub>5</sub>-Na<sub>2</sub>O-CaO-SiO<sub>2</sub> glass-ceramics. *Acta Biomater.* **2012**;8(1):321–332.
- [209] Onbaşlı MC, Tandia A, Mauro JC. Mechanical and compositional design of high-strength Corning Gorilla® Glass. In: Andreoni W, Yip S, editors. *Handbook of materials modeling*. Cham: Springer; **2018**. p. 1–23.
- [210] Mauro JC. Grand challenges in glass science. *Front Mat.* **2014**;1:20.
- [211] Mauro JC, Zanotto ED. Two centuries of glass research: historical trends, current status, and grand challenges for the future. *Int J Appl Glass Sci.* **2014**;5(3):313–327.
- [212] Montazerian M, Singh SP, Zanotto ED. An analysis of glass-ceramic research and commercialization. *Am Ceram Soc Bull.* **2015**;94(4):30–35.
- [213] Liu H, Fu Z, Yang K, et al. Machine learning for glass science and engineering: A review. *J Non Cryst Solids X.* **2019**;4:100036.
- [214] Tandia A, Onbasli MC, Mauro JC. Machine learning for glass modeling. In: Musgraves JD, Hu J, Calvez L, editors. *Springer handbook of glass*. Cham, Switzerland: Springer Handbooks; **2019**. p. 1157–1192.
- [215] De Guire E, Bartolo L, Brindle R, et al. Data-driven glass/ceramic science research: insights from the glass and ceramic and data science/informatics communities. *J Am Ceram Soc.* **2019**;102(11):6385–6406.